Environmental RTDI Programme 2000–2006

CLIMATE CHANGE:

Regional Climate Model Predictions for Ireland

(2001-CD-C4-M2)

Prepared for the Environmental Protection Agency

by

Community Climate Change Consortium for Ireland

Authors:

Ray Mc Grath, Elisa Nishimura, Paul Nolan, Tido Semmler,

Conor Sweeney and Shiyu Wang

ENVIRONMENTAL PROTECTION AGENCY

An Ghníomhaireacht um Chaomhnú Comhshaoil
PO Box 3000, Johnstown Castle, Co. Wexford, Ireland

Telephone: +353 53 60600 Fax: +353 53 60699
E-mail: info@epa.ie Website: www.epa.ie

ACKNOWLEDGEMENTS

C4I is supported and funded by the Environmental Protection Agency (under the National Development Plan), Met Éireann, Sustainable Energy Ireland, and the Higher Education Authority.

This work was carried out in collaboration with the CosmoGrid Project, funded under the Programme for Research in Third Level Institutions (PRTLI) administered by the Irish Higher Education Authority under the National Development Plan and with partial support from the European Regional Development Fund.

Support from Met Éireann staff, particularly those in the IT and Climate and Observations Divisions, is also acknowledged.

The C4I Project was supported by the Meteorology and Climate Centre, University College Dublin. Numerical integrations were carried out on the high-performance computer facility at UCD and at the European Centre for Medium-Range Weather Forecasts (ECMWF) in Reading. C4I is registered as a Special Project with ECMWF.

Support from the Rossby Centre, Sweden, with the modelling work, is also acknowledged.

DISCLAIMER

ENVIRONMENTAL RTDI PROGRAMME 2000–2006

Published by the Environmental Protection Agency, Ireland

PRINTED ON RECYCLED PAPER

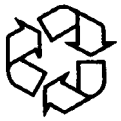

ISBN:1-84095-166-4
Price: €15 05/05/500

Details of Project Partners

Ray McGrath,
Met Éireann,
Glasnevin Hill,
Dublin 9
Ireland

Tel: +353 1 806 5520
Fax: +353 1 806 4247
E-mail: ray.mcgrath@met.ie

Shiyu Wang
Met Éireann,
Glasnevin Hill,
Dublin 9
Ireland

Tel: +353 1 806 5515
Fax: +353 1 806 4247
E-mail: shiyu.wang@met.ie

Paul Nolan
Met Éireann,
Glasnevin Hill,
Dublin 9
Ireland

Tel: +353 1 806 4281
Fax: +353 1 806 4247
E-mail: paul.nolan@met.ie

Elisa Nishimura
Met Éireann,
Glasnevin Hill,
Dublin 9
Ireland

Tel: +353 1 806 5542
Fax: +353 1 806 4247
E-mail: elisha.nishimura@met.ie

Tido Semmler
Met Éireann,
Glasnevin Hill,
Dublin 9
Ireland

Tel: +353 1 806 5535
Fax: +353 1 806 4247
E-mail: tido.semmler@met.ie

Conor Sweeney
Met Éireann,
Glasnevin Hill,
Dublin 9
Ireland

Tel: +353 1 806 5536
Fax: +353 1 806 4247
E-mail: conor.sweeney@met.ie

Peter Lynch
Meteorology and Climate Centre
Mathematical Physics Department
University College Dublin
Belfield
Dublin 4

Tel: +353 1 7162431
Fax: +353 1 7161172
E-mail: peter.lynch@ucd.ie

Table of Contents

Executive Summary

This report provides an analysis of future Irish climate conditions for the period 2021–2060 based on the outputs from a new regional climate modelling facility located in Met Éireann. These are the first results from the Met Éireann Regional Climate Model and represent the first steps in an ambitious programme to run an ensemble of simulations that will improve our understanding of climate change and its implications for Ireland, and quantify the uncertainties in the climate projections. The simulation of the future climate is driven at the boundaries by the output of the Max Planck Institute Global Climate Model with future greenhouse gas concentrations following the moderately increasing concentrations scenario used by the Intergovernmental Panel on Climate Change.

Projected temperature changes from the model output show a general warming in the future period with mean monthly temperatures increasing typically between 1.25 and 1.5°C. The largest increases are seen in the south-east and east, with the greatest warming occurring in July.

For precipitation, the most significant changes occur in the months of June and December; June values show a decrease of about 10% compared with the current climate, noticeably in the southern half of the country; December values show increases ranging between 10% in the south-east and 25% in the north-west. There is also some evidence of an increase in the frequency of extreme precipitation events (i.e. events which exceed 20 mm or more per day) in the north-west.

In the future scenario, the frequency of intense cyclones (storms) over the North Atlantic area in the vicinity of Ireland is increased by about 15% compared with the current climate. This is related to the projected general rise in sea surface temperatures.

In a practical application of this new data set, a hydrological model was used to assess the impact of climate change on river discharge and local flooding in the Suir catchment area. The increase in winter precipitation was found to produce a significant increase in the more intense discharge episodes, raising the risk of future flooding in the area.

As part of the climate model validation work, a 40-year simulation of the past climate (1961–2000) was also completed. The output data complement the archive of existing climate observations and, together with the data for the future climate, greatly enhance the scope for studies of the impacts of climate change in Ireland.

1 Introduction and Outline of Report

1.1 Background

The Community Climate Change Consortium for Ireland (C4I) project has enabled the establishment of a regional climate modelling facility in Met Éireann. A key objective is to develop a new national capacity to forecast future climate conditions in Ireland. This is considered to be necessary for the development of national planning for adaptation to the impacts of projected climate change. This report provides an analysis of the first major output from the C4I regional climate model; it is the first of a series of such reports, which will build on this analysis.

Addressing anthropogenic climate change, caused by the build up of greenhouse gases (GHG) in the atmosphere, is one of the greatest challenges of this century. The work of the Intergovernmental Panel on Climate Change (IPCC) has provided an authoritative analysis of the science of climate change, as well as mitigation and adaptation options, and informs the actions under the UN Framework Convention on Climate Change (UNFCCC).

The IPCC Third Assessment Report (TAR) (IPCC, 2001) has attributed observed warming to anthropogenic influences. More recent reports on climate change show rapid changes in key regions such as the Arctic (ACIA, 2005) and locally in Ireland (Sweeney *et al.*, 2002). It is also recognised that, due to the long atmospheric lifetimes of GHG, climate change impacts will continue to evolve over the coming decades regardless of international actions, such as the Kyoto Protocol to the UNFCCC, to reduce emissions.

To be effective, mitigation actions to reduce emissions of GHG need to be taken at a global level. However, impacts assessment and adaptation measures are largely taken at national and local levels. Effective adaptation actions need to be informed of likely changes and uncertainties in climate projections. Work in the C4I project is a key component in the development of national and local adaptation planning.

1.2 Outline of this Report

A Regional Climate Model (RCM) has been used to create a 40-year simulation of the past climate (1961–2000). This was done to verify that the model is capable of capturing the essential features of the Irish climate at the scale of the model configuration (i.e. on a 0.12° horizontal grid). This produced an extensive data set of surface and upper-air weather parameters for comparison against available climatological observations in the Met Éireann archive. These results are discussed in Chapter 2. An in-depth analysis of the changing precipitation patterns over the 40 years is provided in Chapter 3.

Following the verification of the model performance in recreating the past climate, the model was used to simulate the future climate for the period 2021–2060. The Regional Climate Model was driven by output from the Max Planck Institute ECHAM4 coupled atmosphere–ocean Global Climate Model (GCM). This transient simulation, extending from 1860 to 2100, used observed GHG concentrations up to 1990 and a scenario of moderately increasing GHG concentrations for the future (the Special Report on Emissions Scenarios (SRES)-B2 scenario – see Appendix IV for details). Evaluation of the climate change requires a reference simulation and this was run for the period 1961–2000, again driven by ECHAM4 data. The results are discussed in Chapter 4.

The results of a case study in which a standard hydrological model was used to simulate river discharge in the Suir catchment area are discussed in Chapter 5. The increase in winter precipitation was found to produce a significant increase in the more intense river discharge episodes, raising the risk of future flooding in the area.

Chapter 6 analyses the frequency and intensity of cyclones, and their movement, comparing statistics from the ERA-40 re-analysis data with those from the past simulation. In the future simulation (2021–2060), the frequency of very intense cyclones/storms with core pressures less than 950 hPa, shows substantial changes: a 15% increase compared to a reference simulation with even stronger increases in winter and spring seasons.

2 Simulation of Past Climate

Summary of contents: The regional climate model has been validated by performing a 40-year simulation of the Irish climate (1961–2000), using re-analysis data[1] to drive the model, and the output compared against a wide range of observational data from the Met Éireann climatological archive. Results confirm that the model is able to capture the essential features of the Irish climate. Some systematic differences are observed in the simulation of some weather elements. These do not compromise the ability of the model to simulate the future climate.

2.1 Introduction

The regional climate model used by the C4I project is based on the operational weather forecast model developed by Met Éireann as part of the HIRLAM Project and further refined by the Rossby Centre climate modelling research unit at Swedish Meteorological and Hydrological Institute (SMHI) (Rummukainen *et al.,* 2001). Initial studies showed that while the dynamical downscaling is sensitive to the domain size and orientation for specific weather events, for climate evaluation the sensitivity was marginal for the range of domains used in the original assessment work. Accordingly, the choice of domain for validating the model and for generating future climate scenarios was based primarily on two factors: computational economy, and the desirability of having the lateral boundary zones away from areas of steep orography while sufficiently far away from Ireland to reduce errors (see Appendix I for a more general description of regional climate modelling and further details regarding the model configuration).

This domain, shown in Fig. 2.1, is based on a rotated grid system with 156 × 166 grid points in the horizontal, corresponding to a resolution of about 0.12° (approximately 13 km) over Ireland. In the vertical extent, there are 40 unequally spaced levels.

The rationale for the validation exercise is to ensure that the model is capable of reproducing the essential features of the Irish climate and to reveal any significant deficiencies. For this purpose, the European Centre for Medium-Range Weather Forecasting (ECMWF) ERA-40 global re-analysis data (Uppala *et al.,* 2005) were used to drive the model, producing a dynamically downscaled simulation of the climate for the period 1961–2000. The actual simulation was launched from 1959 to allow time for the soil moisture to 'spin up'.

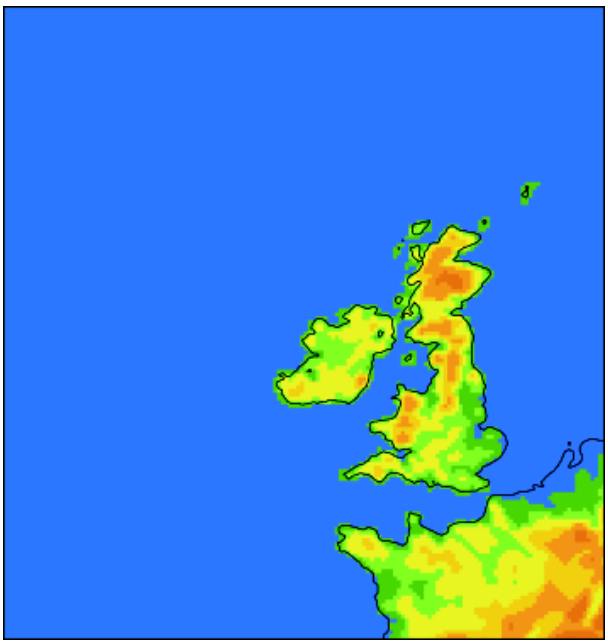

Figure 2.1. Model domain.

The simulation produces a wide range of meteorological products, listed in Appendix III, delivered with a 3-h frequency.

2.2 Verification

To verify the outputs, three data sources were exploited:

1. United Kingdom Climate Impacts Programme (UKCIP) data, a data set that includes monthly averages of 2-m temperature and monthly total precipitation, on a 5 km grid covering Ireland.
2. The Met Éireann climate archive, containing detailed information from the Irish synoptic and climate stations.
3. Satellite data from the Hamburg Ocean Atmosphere Parameters and Fluxes from Satellite Data (HOAPS) database.

The ERA-40 re-analysis fields are also available. For validation, the simulation fields were either transformed to

1. The ERA-40 re-analysis data are described in Appendix II.

the UKCIP grid or spatially interpolated to the locations of the stations.

In this report, only the essential validation results are presented; further information can be found on the C4I web site (http://www.c4i.ie).

Verification results for Ireland, based on the Irish observational data and the UKCIP and ERA-40 fields, are presented in Section 2.3. Section 2.4 discusses the validation over sea using satellite data from the HOAPS database.

2.3 Validation over Ireland

2.3.1 *Mean sea level pressure (MSLP)*

Figure 2.2 shows the average of the MSLP fields over the model domain for the simulation period 1961–2000: (a) RCM data, (b) ERA-40 data, and (c) the mean difference. Relative to the reference ERA-40 data the large-scale circulation pattern is captured quite well by the model; there is a slight negative bias centred over England but the maximum difference is within 0.5 hPa of the ERA-40 values.

2.3.2 *Temperature, radiation and cloud cover*

Figure 2.3 shows the validation results for the average January 2-m temperature from 1961 to 2000: (a) ERA-40 re-analysis data, and (b) differences relative to UKCIP; (c) RCM, (d) and differences relative to UKCIP. The model is in much better agreement with the observed temperatures (i.e. UKCIP) than with the ERA-40 data. The main differences for the model occur around the coast and in some mountainous areas but overall are small (areas marked in white are within 0.25°C of observations). Differences near the coast could be due to a lack of observational data and a consequent poor interpolation for the UKCIP data; those in mountainous areas could be partially attributed to the relatively crude (0.12°) representation of the orography by the model. Results for other months are very similar.

Figure 2.4 shows the yearly 2-m temperature time series for Valentia from 1961 to 2000. The inter-annual variability is captured well by the model, as are the longer-term trends. The 5-year running average values, plotted in bold, show an increase in temperature up to 1975, followed by a cooling to 1986, and a marked increase towards the end of the century.

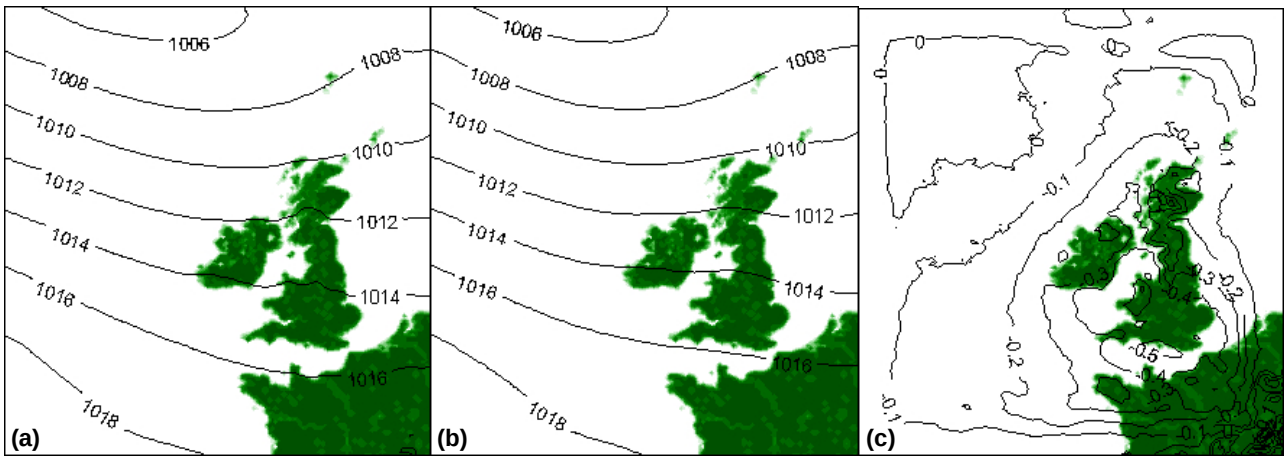

Figure 2.2. Verification of the Regional Climate Model. The mean sea level pressure field is a sensitive indicator of the atmospheric flow. The ERA-40 data are based on weather observations and therefore provide a measure of the true state of the atmosphere on scales in excess of about 125 km. These data, available at 6-h intervals, drive the climate model, the information flowing through the lateral boundaries. In the interior of the domain, the model has freedom to develop it own climate, unconstrained by observations, but ideally should not affect the large-scale flow pattern of the ERA-40 data; the main impact should be in the smaller scales related to the resolution of the climate model, i.e. in the range 13–125 km. Averaged over the simulation period 1961–2000, for (a) the climate model simulation data and (b) ERA-40 data, the plots show good agreement (mean difference in (c)). Units are in hPa.

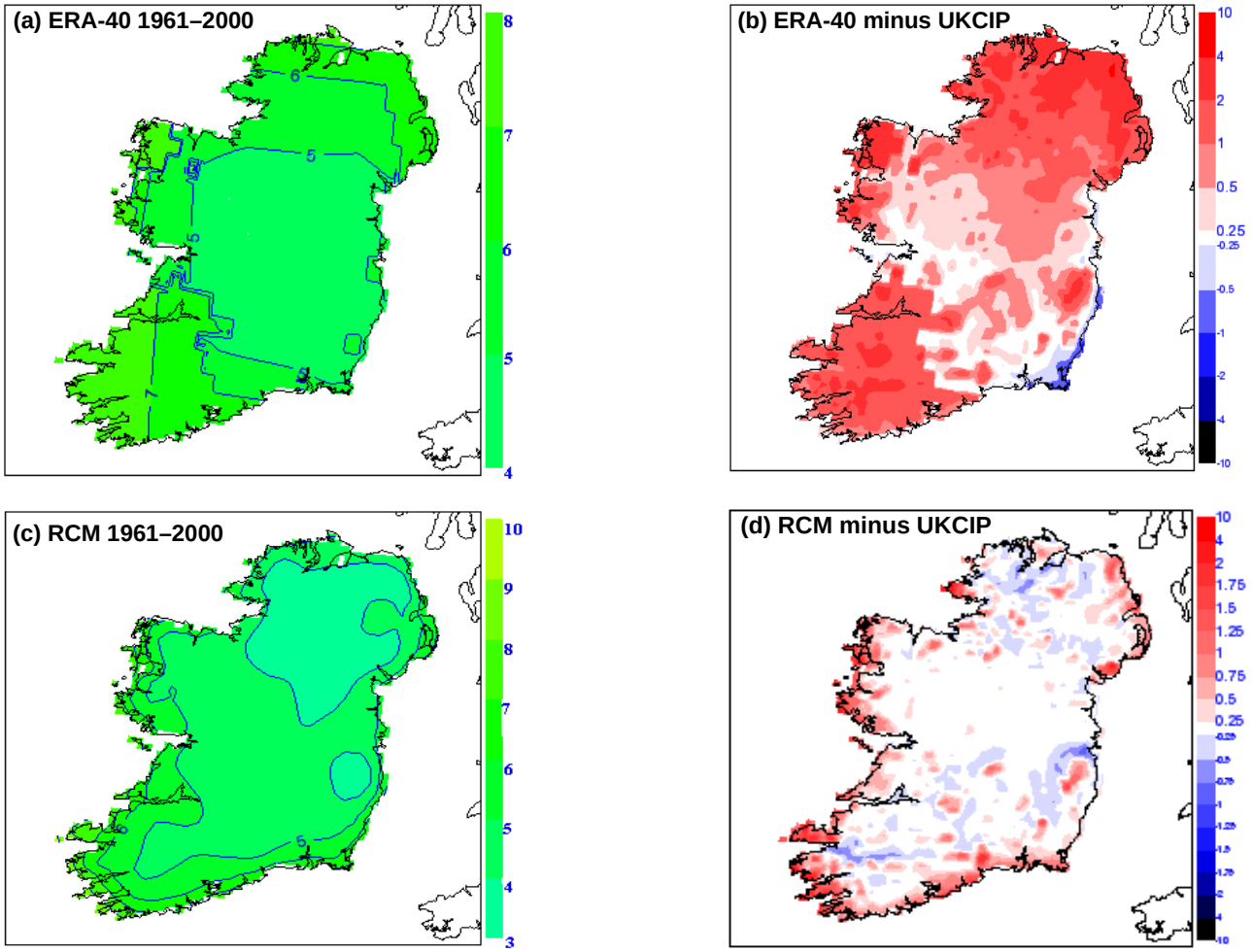

Figure 2.3. Regional Climate Model verification. The temperature measured at 2-m height (i.e. the standard meteorological temperature) is difficult to model. The ERA-40 data, while based on meteorological observations, do not accurately reflect the regional variation in observed temperatures, mainly because of the relatively coarse resolution (around 125 km) of the global model; surface elevations in the model are average values, the averages taken over an area with a size reflecting the resolution. This will be particularly true in mountainous areas. Therefore, the UKCIP data are used for verification; these data are based on observed temperatures interpolated to a 5-km grid covering Ireland. The impact of the higher resolution of the RCM compared with the ERA-40 (global) model is clearly seen in the difference plots (b) and (d) for the average January (1961–2000) temperature. Results are similar for other months.

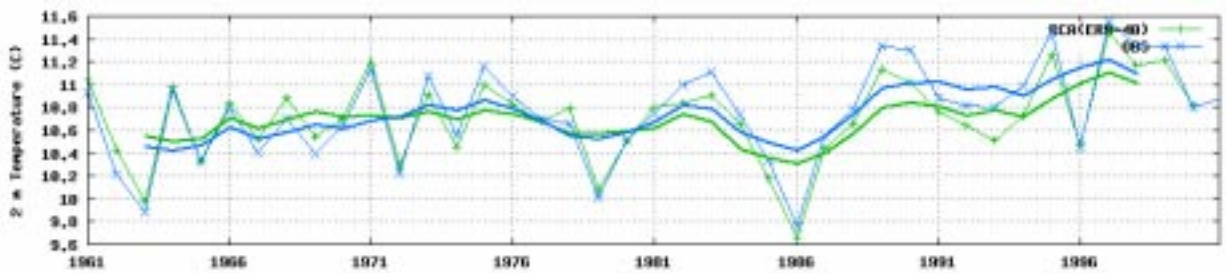

Figure 2.4. Regional Climate Model verification: variation of the annual mean 2-m temperature at Valentia Observatory for the period 1961–2000. Observed values are shown in blue, RCM values in green; 5-year running average values are highlighted in bold.

The yearly time series of short-wave radiation at the surface and total cloud cover are also shown (Fig. 2.5). In the case of the radiation, the model values are systematically too high compared to the observations and, while the patterns in the 5-year running average values are broadly similar, the model fails to catch the slow decline in the observed values over the period. The long-term reduction in the observed radiation ('global dimming') is an intriguing feature that has been the subject of several studies (e.g. Stanhill, 1998) and may be related to increases in atmospheric aerosols due to increasing pollution emissions in this period. However, the model has a fixed set of parameters to calculate the radiation effects of aerosols, which may explain the lack of a trend in the simulated data.

To investigate the diurnal cycle of temperature, decadal monthly averages were calculated based on 3-h values from both the observation and simulation data. Figure 2.6 shows the results for Kilkenny for January and July in the 1960s and 1990s. The model slightly underestimates the range of the cycle in January, and overestimates the maximum temperature in July in the 1960s. However, both the model and observations show a shift towards warmer temperatures from the 1960s to the 1990s, and the amplitude of the diurnal cycles are generally well reproduced.

2.3.3 Precipitation

Sample results for the average monthly precipitation for the representative months of January and April are shown in Fig. 2.7. The plot for January shows that rainfall in the midlands is overestimated by about 20% in comparison with observational data. Two factors may have contributed to this: the observations generally

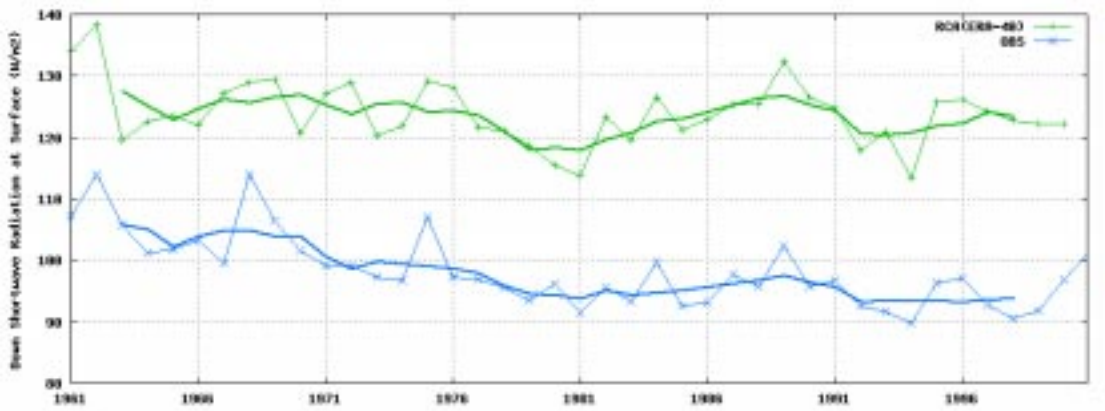

(a) Solar radiation

(b) Cloud cover

Figure 2.5. Regional Climate Model verification: variation of the annual mean solar radiation (a) and cloud cover (b) at Valentia Observatory for the period 1961–2000. Observed values are shown in blue, RCM values in green; 5-year running average values are highlighted in bold. Note the slow decline in the observed solar radiation.

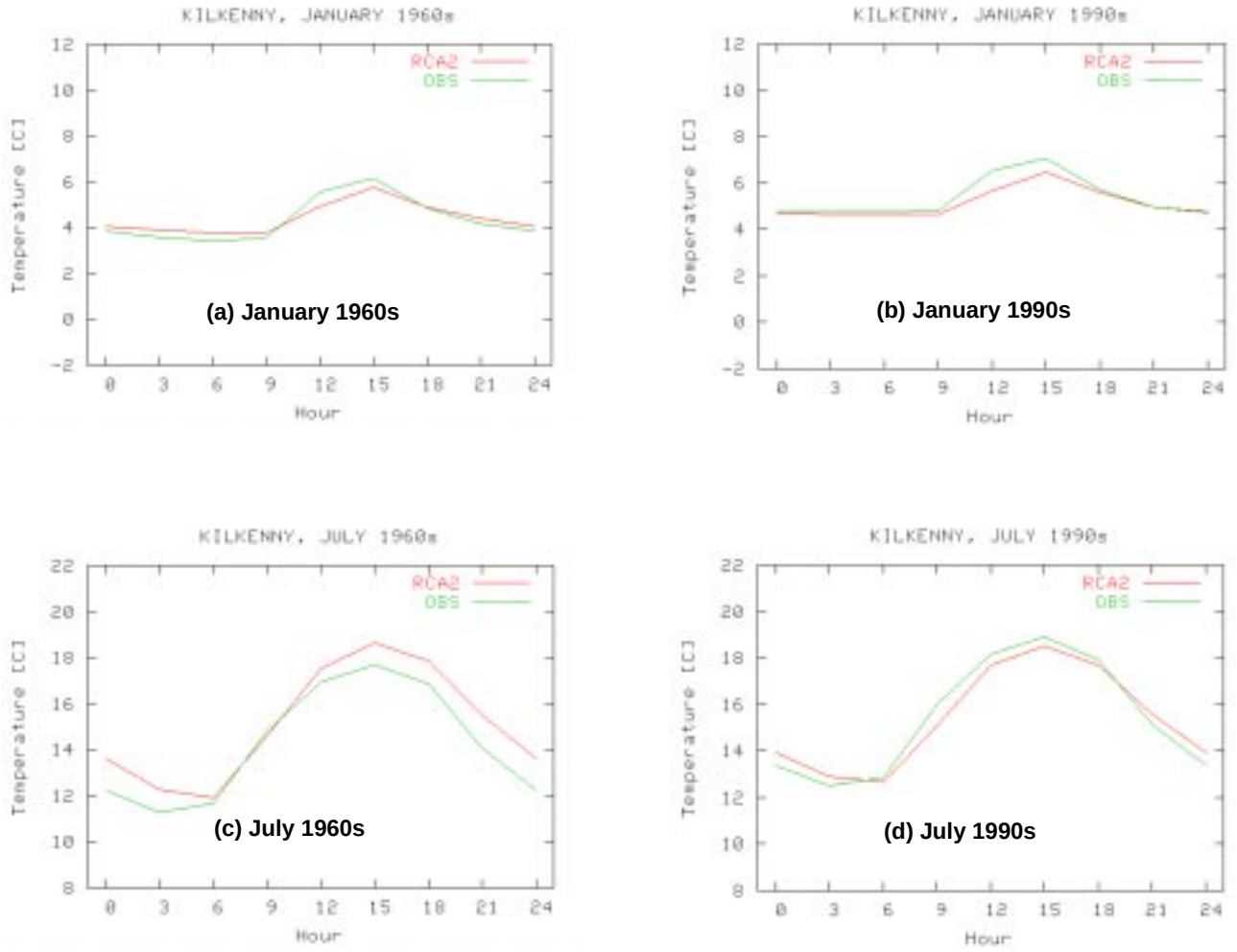

Figure 2.6. Regional Climate Model verification: diurnal cycle of temperature change. Observed 3-h mean 2-m temperatures for Kilkenny for January and July are shown in green, with RCM values in red.

underestimate rainfall amounts, particularly in windy conditions, and the model may produce too many light precipitation events. In contrast, there is too little rainfall in mountainous areas, where the model underestimates rainfall by up to 15%. This could be attributed to a lack of detail in the representation of the surface features at the 0.12° resolution of the model.

Agreement between the model and observations is better in April, a drier month. Overall, there is an overestimation of rainfall, probably due to an excess of low precipitation events. Agreement in mountainous areas is better, however, suggesting that only the heavy rainfall over the mountains is difficult to simulate.

The yearly precipitation time-series plot for Belmullet (Fig. 2.8) shows that the inter-annual variability and time trend are well reproduced. The model shows a consistent positive bias, as was seen in the monthly plots.

The number of dry days per year (<0.2 mm) for Belmullet is plotted in Fig. 2.9a. The tendency of the model to over-predict small amounts of rain is clearly seen in the data. However, both the model and observations show that the number of dry days has not changed much over the simulation period. The annual number of days with heavy rainfall (24-h total exceeding 20.0 mm) is shown for Belmullet in Fig. 2.9b. Here, the model is in good agreement with observations, with both showing an initial decrease in the 1960s, followed by an increasing trend. A more detailed analysis of the simulated precipitation data is presented in Chapter 3.

2.3.4 Wind

Figure 2.10 shows the yearly 10-m wind speed for Belmullet. The peaks and troughs in wind values from year to year are captured well by the model, although the

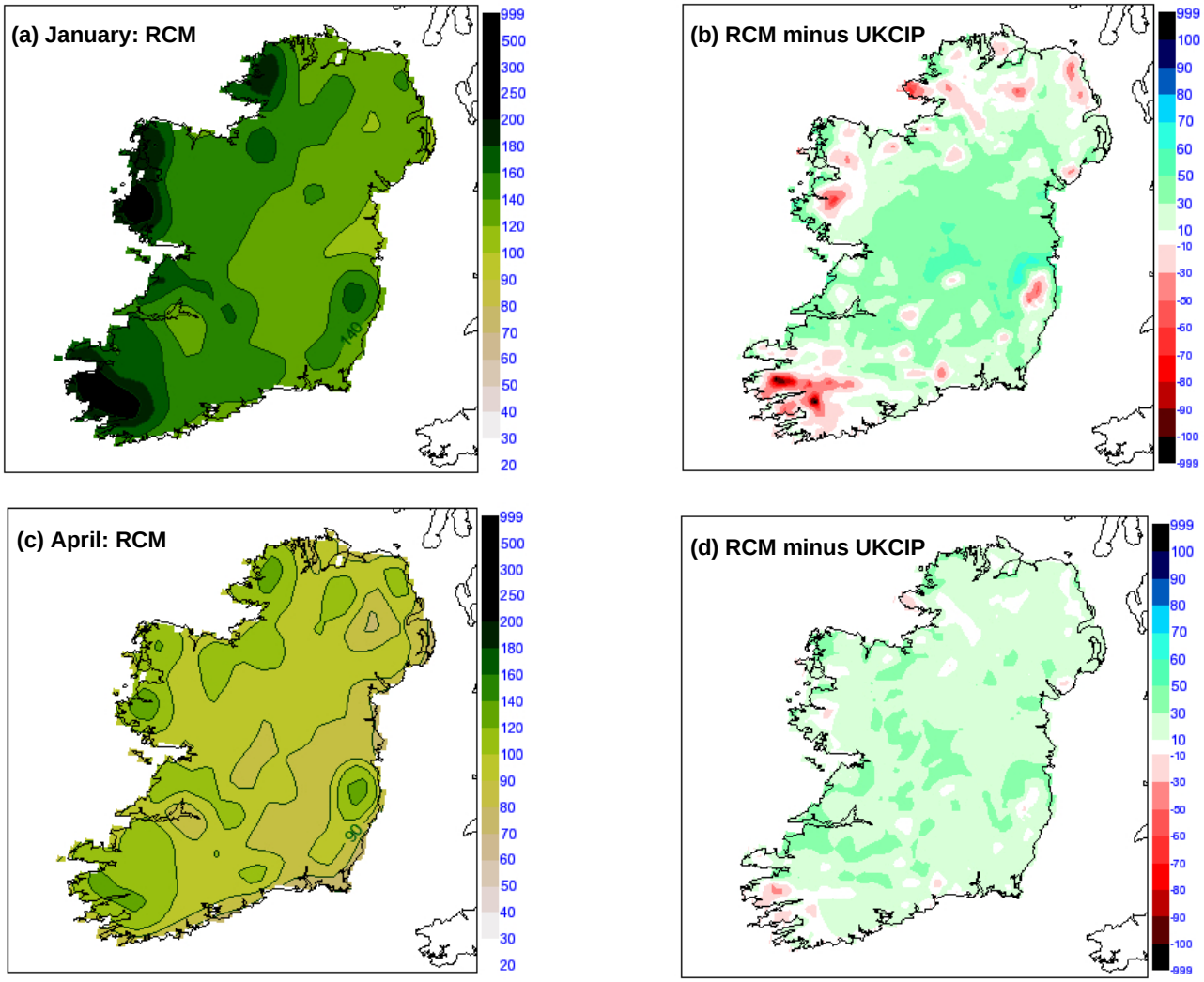

Figure 2.7. Regional Climate Model verification. Mean monthly precipitation (1961–2000) for January (a) and April (c) and differences relative to the UKCIP data ((b) and (d)). The UKCIP data are based on observed precipitation values interpolated to a 5-km grid. Units: millimetres.

Figure 2.8. Regional Climate Model verification: variation of the annual mean precipitation for Belmullet for the period 1961–2000. Observed values are shown in blue, RCM values in green; 5-year running average values are highlighted in bold.

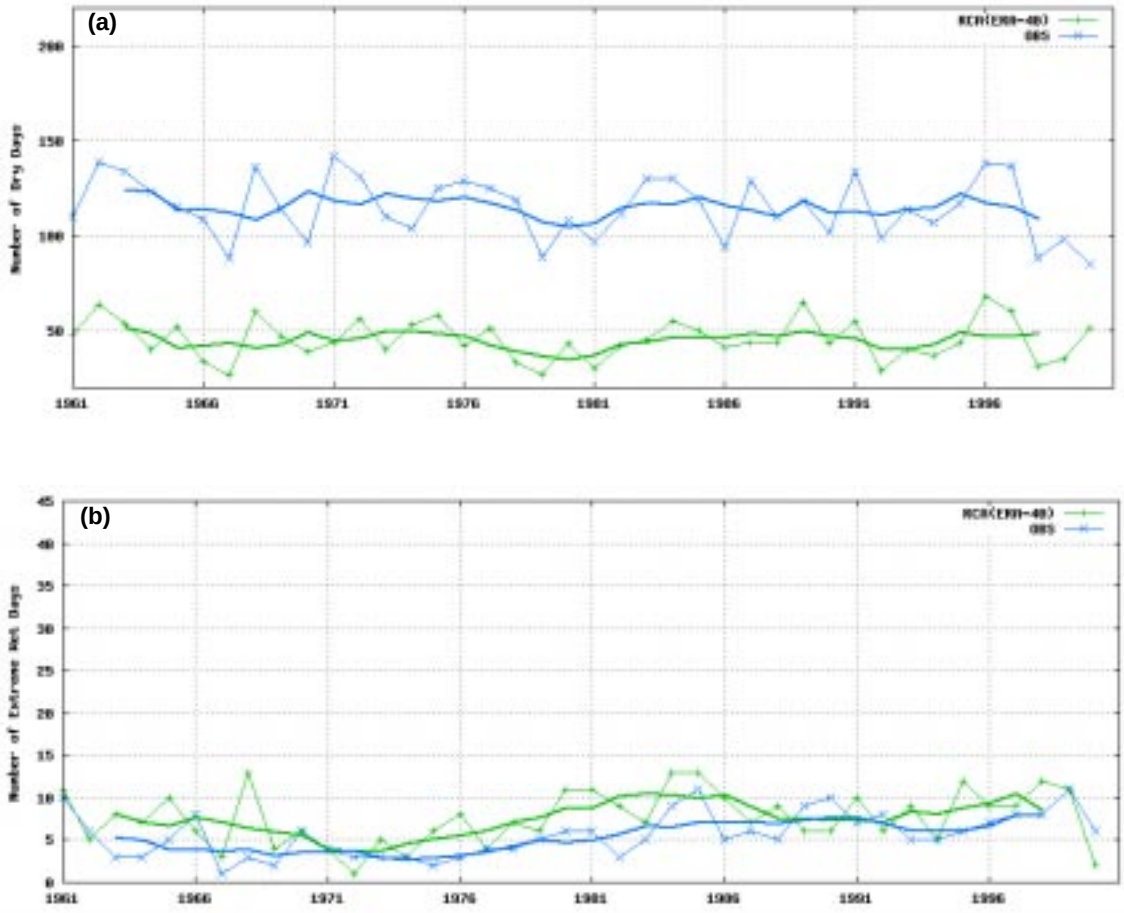

Figure 2.9. Regional Climate Model verification: variation of the annual mean number of dry days (<0.2 mm/day) (a) and heavy rainfall days (>20.0 mm) (b) for Belmullet for the period 1961–2000. Observed values are shown in blue, RCM values in green; 5-year running average values are highlighted in bold.

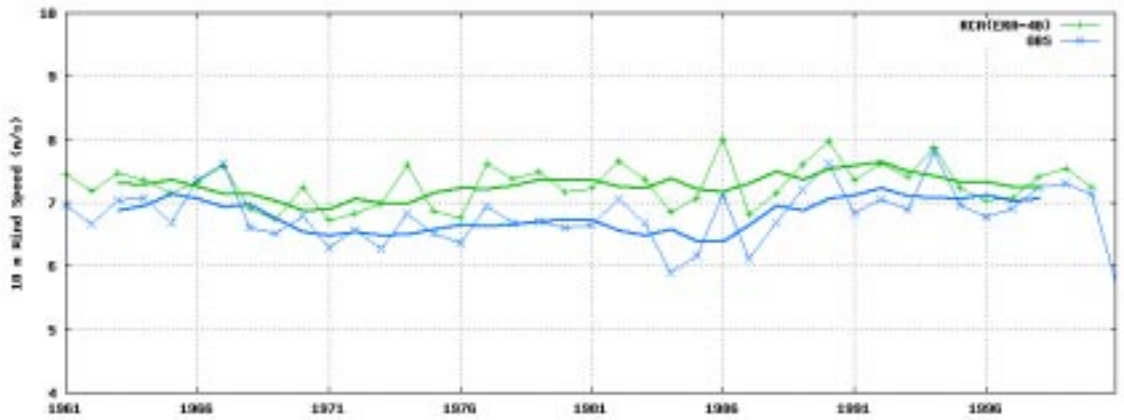

Figure 2.10. Regional Climate Model verification: variation of the annual mean wind speed at 10-m height for Belmullet for the period 1961–2000. Observed values are shown in blue, RCM values in green; 5-year running average values are highlighted in bold.

model winds are generally stronger than the observed values. Similar results are found for other stations.

2.4 Validation over the Ocean

The North Atlantic Ocean plays a predominant role in determining the Irish climate; any changes in this region may have significant impacts for Ireland and other areas of Europe. It is therefore vital to include the sea areas in the model validation. However, compared with land areas, surface observations (mainly reports from ships and buoys) are sparse and data quality is also a significant issue. This is a key topic for the understanding of current weather patterns and future climate issues for Ireland, and an advanced programme to enhance and develop additional necessary observational capacity in this region is needed. Fortunately, the HOAPS archive (see Appendix III for a description) has an extensive set of derived meteorological parameters, based on satellite measurements, over the sea areas; this was used to supplement the surface observations for validating the model.

The following products, generated from the last decade of the 40-year regional climate simulation (1991–2000), were validated using this database: the vertically integrated water vapour, 10-m wind speed, net long-wave radiation, sensible and latent heat fluxes. The vertically integrated water vapour was also compared against the ERA-40 data as this parameter is assimilated from observations in the re-analyses.

The spatial distribution of the vertically integrated water vapour is very similar in all three data sets (Fig. 2.11). However, particularly in the summer months, the water vapour content is slightly higher both in the ERA-40 and

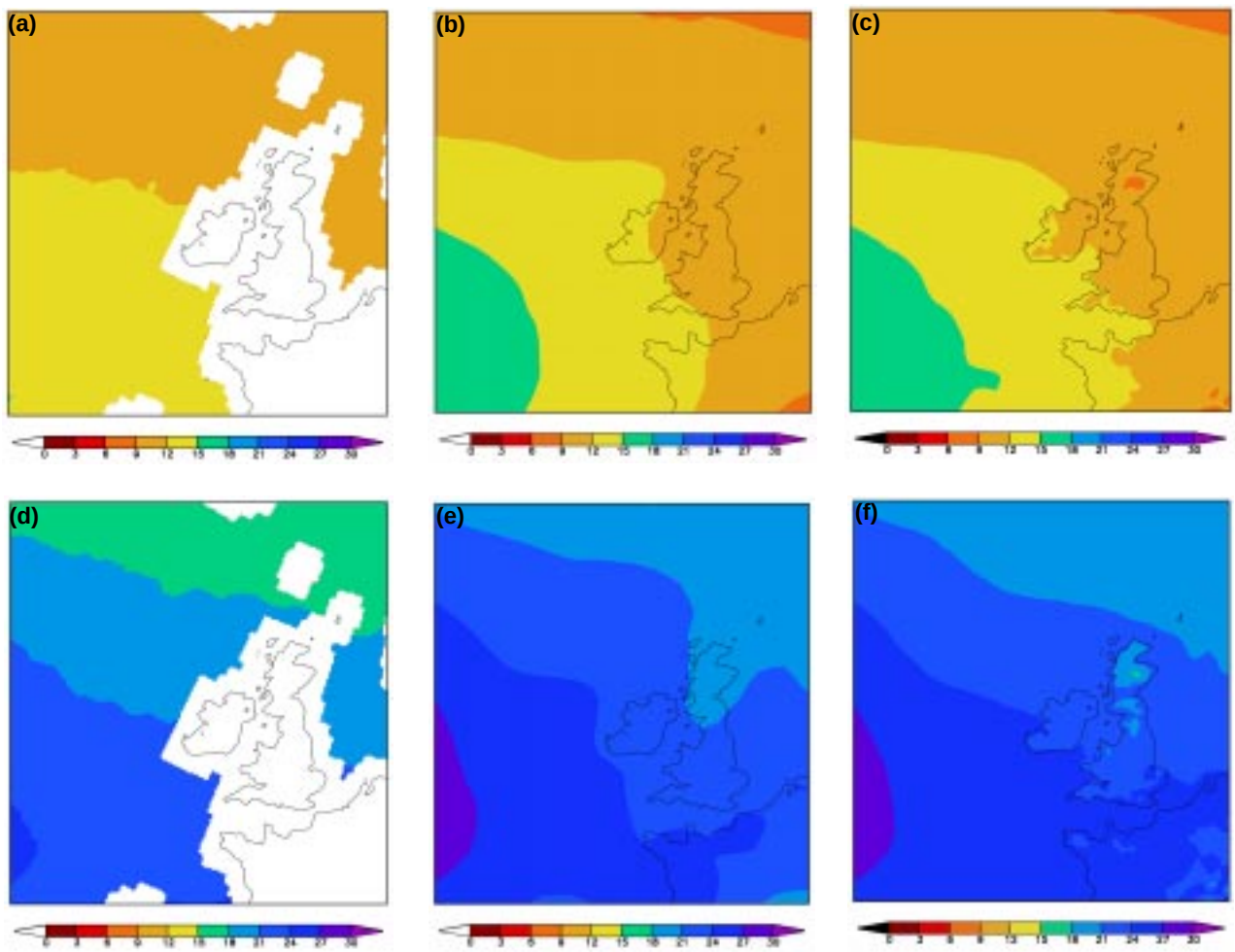

Figure 2.11. Verification of the Regional Climate Model: vertically integrated water vapour (kg/m^2) as decadal monthly means for January 1991–2000 from (a) HOAPS, (b) ERA-40 and (c) the RCM. Plots (d) to (f) show the equivalent data for July 1991–2000. Note that the HOAPS data are only available over the sea area.

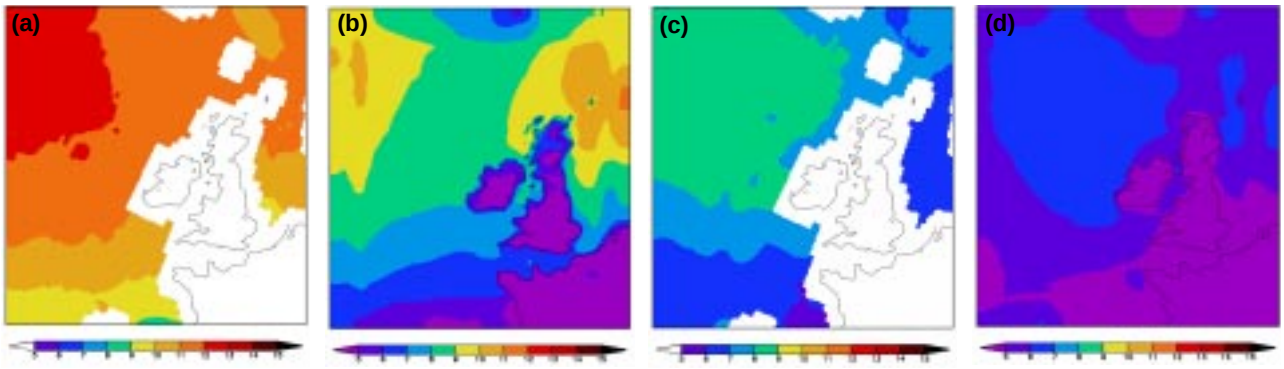

Figure 2.12. Verification of the Regional Climate Model: 10-m wind speed (m/s) as decadal monthly means for January 1991–2000 from (a) HOAPS and (b) the RCM. Plots (c) and (d) show the equivalent data for July 1991–2000. Note that the HOAPS data are only available over sea areas.

RCM data compared to HOAPS. The RCM bias is not unexpected as the model humidity is driven by the ERA-40 data. The slight overestimation in summer may explain the overestimation of precipitation in this season.

The spatial distribution of the 10-m wind speed shows a good agreement between the RCM and HOAPS data (Figure 2.12). However, the speed is systematically underestimated by 3 to 4 m/s in winter and 2 m/s in summer.

A scatter plot of the RCM simulated wind speed and the observed data from the K2 ocean buoy at 51° N, 13.3° W shows that the RCM winds have a small systematic positive bias but otherwise the fit is quite reasonable over the range of speeds encountered (Fig. 2.13). This is slightly at odds with the HOAPS data which suggests that the model wind speeds are underestimated.

The discrepancy may be explained by the fact that the ocean buoy measures the wind speed at a height of 3 m instead of at the standard height of 10 m, i.e. observed values are a little too low. However, it is difficult to draw general conclusions from a single site. The accuracy of the satellite derived 10-m wind speed is given as 1.4 m/s (Schulz *et al.,* 1997) and hence does not explain the difference.

The latent heat fluxes (Fig. 2.14) are very well represented in our model simulation. The differences (slightly stronger negative heat fluxes in the RCM compared to HOAPS) are within the uncertainties of the satellite data. Also, the net long-wave radiation is well simulated. It is a little less negative than in HOAPS (Fig. 2.15), which might be connected to the slightly overestimated water vapour content.

2.5 Conclusions

The validation results confirm that the RCM is effective in simulating the essential features of the Irish climate. While there is evidence of systematic differences relative to observations for some weather elements, it does not compromise the ability of the model to simulate the future climate.

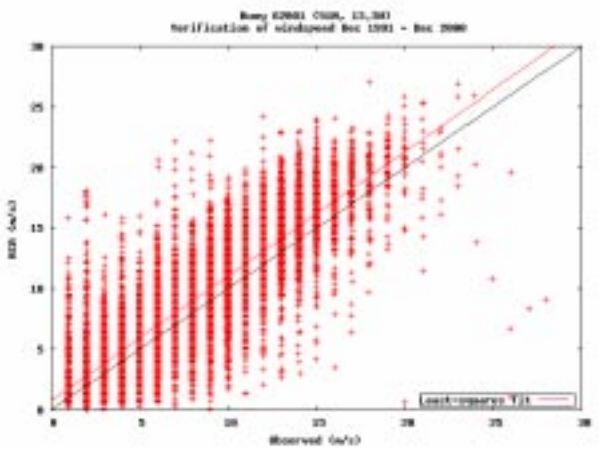

Figure 2.13. Scatter plot of the observed wind speed from ocean buoy 62081 (51° N, 13.3° W) for December 1991 to December 2000 compared to the Regional Climate Model output. Buoy measurements are at a height of 3 m whereas the model output is at a height of 10 m (results interpolated to the location of the buoy). The red line indicates the linear least-squares fit.

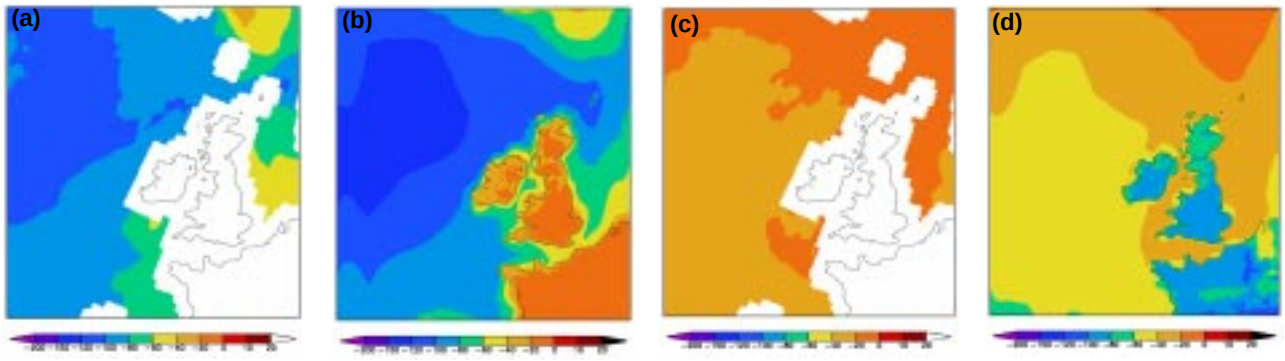

Figure 2.14. Verification of the Regional Climate Model: latent heat flux (W/m) as decadal monthly means for January 1991–2000 from (a) HOAPS and (b) the RCM. Plots (c) and (d) show the equivalent data for July 1991–2000. Note that the HOAPS data are only available over sea areas.

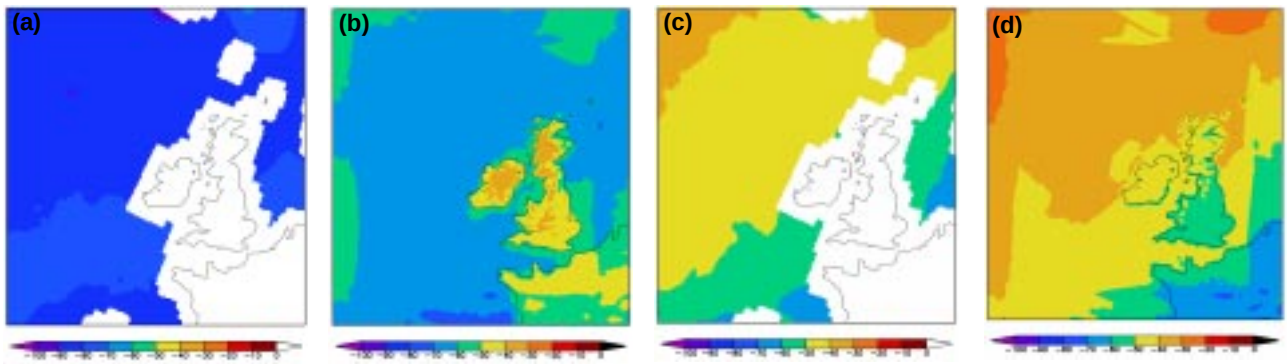

Figure 2.15. Verification of the Regional Climate Model: net long-wave radiation (W/m) as decadal monthly means for January 1991–2000 from (a) HOAPS and (b) the RCM. Plots (c) and (d) show the equivalent data for July 1991–2000.

3 Validation of Simulated Precipitation Patterns over Ireland for the Period 1961–2000

Summary of contents: An advanced statistical method was used to analyse the annual and interannual variability of the precipitation patterns over Ireland, as simulated by the Regional Climate Model, for the period 1961–2000. The annual and monthly precipitation results show that, compared with observations, the model captures the major spatial patterns for this period although the seasonal cycle in the simulation is less pronounced. Spatial analysis of the monthly precipitation over the 40-year period shows two major patterns. The first, showing a precipitation maximum in the south-west, is well simulated; the second, showing a maximum in the west and north-west shows a strongly increasing trend, which is slightly underestimated in the model simulation. Both patterns show seasonal and interannual variability, the latter being the more important feature. In general, the model captures the major spatial and seasonal patterns observed between 1961 and 2000 but slightly over-estimates monthly average precipitation levels.

3.1 Introduction

Any model that aspires to provide useful guidance on future climate change must be capable of realistically simulating the current and past climate. However, reproduction of the strong spatial and temporal variability of precipitation over Ireland is a challenging modelling task, especially given the intensity of extreme events. Ireland, in spite of its relatively high latitude, has a temperate maritime climate thanks to the warm North Atlantic current, the impact of which is most noticeable along the west coast. The prevailing westerly winds and the local orography to a large extent determine the precipitation patterns for the country (Keane and Collins, 2004), with the highest values generally occurring in regions with high orography.

Precipitation, measured over a long period, is rather evenly distributed throughout the year over Ireland. However, there is considerable temporal and spatial variability if the focus is shifted to short time periods. In a principal component analysis (PCA) of monthly precipitation between 1941 and 1970, for example, Logue (1984) found that with data expressed as percentages of the annual average, the leading principal component (PC1) is a measure of a tendency for rainfall to be higher in summer compared to winter and has a maximum in the midlands and north-east of the country. The second component (PC2) shows a tendency for the first half of the year to be relatively wet and the second half relatively dry; it has a maximum in the south-east.

3.2 Observed Trends and the North Atlantic Oscillation

The pressure distribution over the North Atlantic Ocean, which can be characterised by the North Atlantic Oscillation (NAO) Index, influences the strength of the surface westerly flow (Rogers, 1985). The link between the NAO and precipitation over Europe has been investigated in many previous studies (Rex, 1951; Namias, 1964; Moses *et al.*, 1987; Wilby *et al.*, 1997; Davies *et al.*, 1997). Also, the evaluation of the atmospheric moisture budget reveals coherent large-scale changes since 1980 (Hurrell, 1995). Kiely *et al.* (1998) and Kiely (1999) studied the changing precipitation climate in Ireland and identified 1975 as a significant year (coinciding with the evolution of the NAO): after 1975, the mean precipitation increased as well as the number of extreme precipitation events. The most pronounced increase in the number of extreme precipitation events occurred in August, September and October. In the monthly mean precipitation, there are abrupt increases in March and October after 1975. Investigations of precipitation variation in the decades after 1970 were also carried out by McElwain and Sweeney (2003). They studied the recent trends in temperature and precipitation using Irish observation data. The analysis of the precipitation changes supports the findings of the UKCIP with evidence of a trend towards a winter increase in the north-west of the country and summer decreases in the south-east. In general, the changes are consistent with the summary in the IPCC report (IPCC, 2001) that precipitation amounts have increased by 0.5–1% every decade in the mid/high latitudes of the Northern Hemisphere in the 20th century.

3.3 Experiment Design and Analysis Procedure

3.3.1 Model set-up and data sets

A description of the RCM set-up used for the 40-year (1961–2000) climate simulation can be found in Chapter 2. In this study, simulated monthly precipitation values were evaluated against gridded observation data for Ireland from the UKCIP; the data are available on a grid with a horizontal resolution of 5 km. Monthly and annual precipitation anomalies, normalised by the corresponding standard deviation, were calculated for both the simulation data and observations for the full time series.

3.3.2 Analysis procedure

3.3.2.1 REOF analysis

An advanced statistical technique, using rotated empirical orthogonal functions (REOF) and PCA, was used to analyse the data. This is a widely used method for the analysis of spatial or temporal patterns of various meteorological parameters (Horel, 1981; Richman, 1986, 1987; Jolliffe, 1987; Kawamura, 1994; Chen *et al.*, 2003).

The REOF method, applied to sequences of annual and monthly mean precipitation values at each land grid point, reveals patterns that highlight the spatial characteristics of the precipitation anomaly. In a variation of the method (the so-called non-standard method), the spatial and temporal elements (here mean monthly precipitation values) are swapped in the analysis to show a temporal pattern. For the non-standard method, the original (not normalised) data were used. In addition, another technique known as wavelet analysis was used to analyse the seasonal and inter-annual variability (Torrence and Compo, 1998); results from this method are not presented in this article.

3.4 Results

3.4.1 The spatial pattern of annual and monthly anomalies

Results for the annual mean precipitation data are shown in Fig. 3.1. The main component of the regional spatial pattern is generally well simulated by the RCM when compared against the UKCIP observations.

The mean values of precipitation are subject to seasonal variation although spatial distribution details (location of maxima and minima) are relatively stable (Keane and Collins, 2004). However, local differences in the spatial distribution between individual months must not be overlooked. For most months, the simulation captures the spatial characteristics of the precipitation pattern, at least for the main component. In general, agreement between the RCM and observations is better in the wet winter season (see, for example, the January data in Fig. 3.2) compared with the dry summer season. In the observation record, there is a fast transit from the wet to the dry season in spring, which is too slow in the simulation. Also, in autumn the transition from the dry to the wet season is slower in the simulation than in the observations. The simulated spatial pattern of November is very different from the observed one and is very similar to the simulated October pattern.

Figure 3.3 shows the relative importance of the main component in the pattern analysis for the different months. In the dry season, the main component has less of an influence compared with the wet season. The difference between winter and summer is larger in the observation analysis than in the simulation analysis. Thus, in summer there is more spatial variability in the observation analysis than in the simulation analysis. A reason for this could be the occurrence of more convective precipitation in the summer months than in the winter months.

In general, the model has a less pronounced seasonal cycle in the spatial variability than the observations.

3.4.2 Spatial pattern evolution

The analysis of the monthly and annual data shows that the model largely captures the main features of the precipitation pattern. Here we focus on the time evolution of the monthly data using the same analysis technique (Fig. 3.4). The main component in the analysis shows a maximum in the south and south-west of the country, with good agreement between the RCM and observation data, although the simulation data tend to have more precipitation over the country on average. The simulation values are a little weaker than the ones from the observations in the south-western rainfall maximum, while the simulated rainfall is a little stronger in the midlands. The second pattern shows precipitation maxima located in the west and north-west of the country (Figs 3.4b and 3.4d). In general, the simulation data show the same deficiencies as in the first pattern: the simulated precipitation maxima are less pronounced than in the observation analysis.

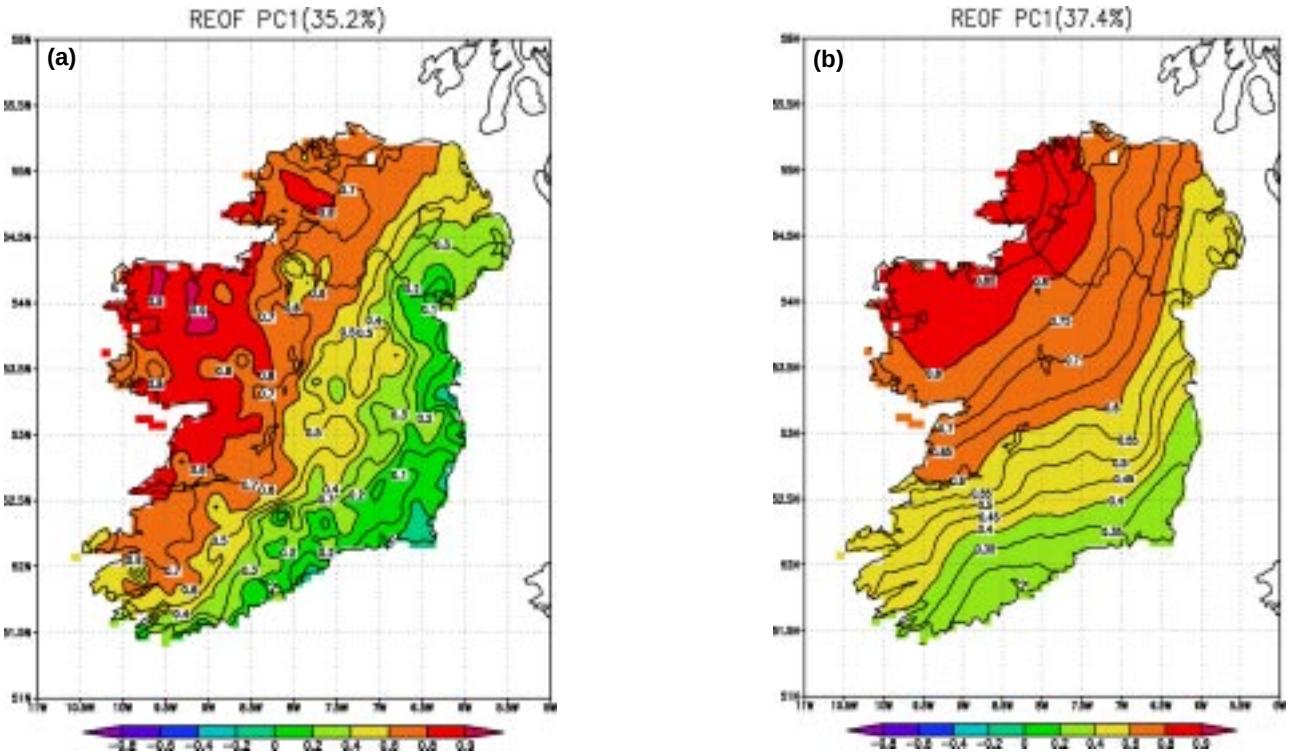

Figure 3.1. The regional, seasonal and long-term variation in precipitation patterns are difficult to analyse. If we focus on the annual mean values for the period 1961–2000 then we have 40 sequences of values for each land point – a considerable amount of data to assess when comparing the output from the Regional Climate Model against observed (e.g. UKCIP) data. As the data sequences are correlated, a principal component analysis is used to simplify the analysis: the data are reorganised into components that are independent, each of which 'explains' a proportion of the variance or spread in the data. The principal components (PCs) are ordered in terms of influence or contribution to the variance. Typically, the essential features of the data can be expressed in the first few PCs and the remainder ignored, thereby simplifying the analysis. The first or leading PC is shown for the observed (a) and simulated (b) annual normalised precipitation, i.e. anomaly values: positive values (e.g. shaded red) indicate values in excess of the annual average, negative values below the average. The importance of the PC is indicated by its contribution to the data variance (35.2% and 37.4% for the model and observations, respectively). Note that the model anomalies are positive except for some small patches along the east and south-east coasts; the largest positive values are located in the north-west and west regions. In the second PC pattern (not shown) for the observations, accounting for 29.4% of the total variance, the largest positive anomaly value is located in the north-west of the country, with negative values elsewhere, especially in the south-east. This pattern is likely to be more pronounced in later data according to McElwain's (2003) analysis of Malin Head (north coast) precipitation data which shows an increasing trend from the late 1970s, possibly connected with the evolution of the NAO index. The third spatial pattern (not shown) shows a negative anomaly over the whole of Ireland with the largest negative value located over the north-east of the country. The fourth and fifth spatial patterns explain very little of the variance; more than 80% is explained by the first three components. In general, agreement between the model and observations is quite good for the leading PC, less so for the higher PCs.

The weight or relative loading as a function of time for the first and second component is shown in Fig. 3.5. Before 1975, the precipitation amount of the first component is relatively small, except for a few peak values (Fig. 3.5a); after 1975, the contribution from this component is generally higher than before 1975 and shows a pronounced decadal variability. The time evolution of the second pattern is different from that of the first pattern

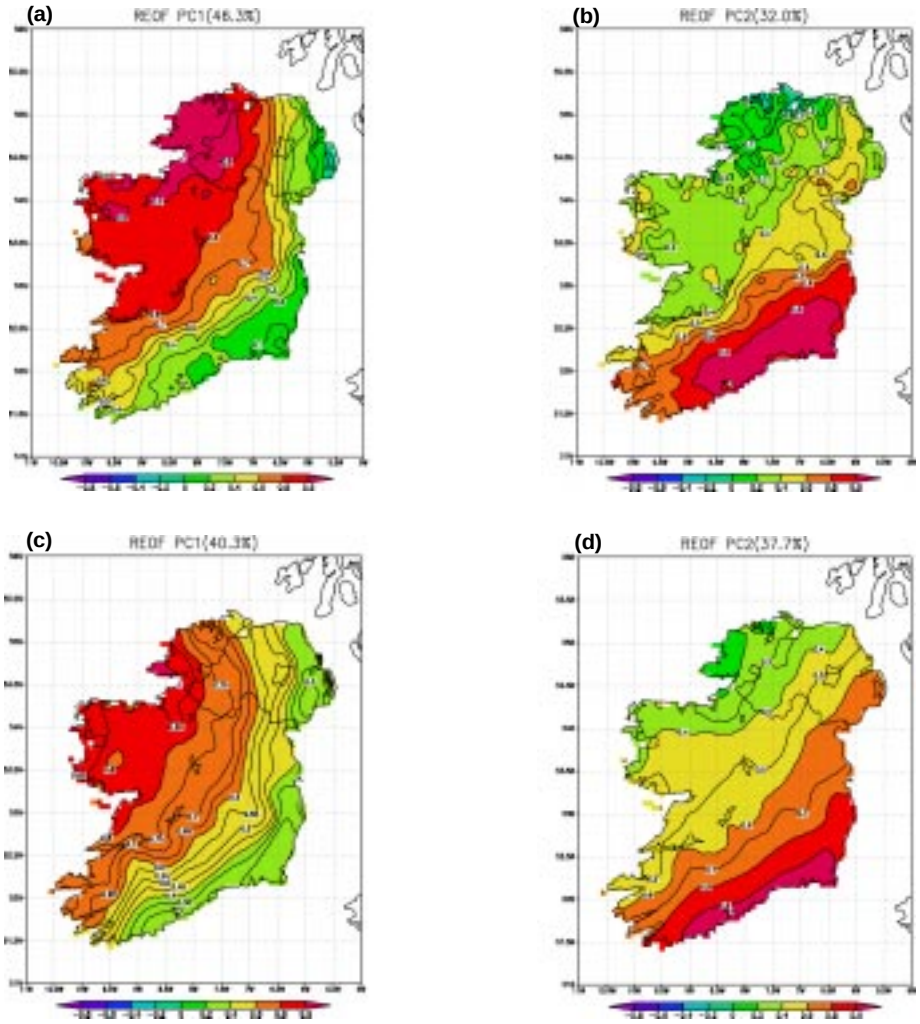

Figure 3.2. Principal component analysis of monthly mean precipitation values for January. The first and second components (PC1 and PC2) for the observations (top) and Regional Climate Model data (bottom) are shown. Positive values (e.g. shaded red) indicate values in excess of the annual average, negative values below the average. Agreement for both components (accounting for around 70% of the variance) is quite good. Note that PC1 is quite similar to the annual spatial precipitation pattern (Fig. 3.1a); its distribution reveals strong gradients with high values in the north-west of the country and lower values in the south-east. Agreement between the model and observations is generally better in the wet winter months compared with the summer months.

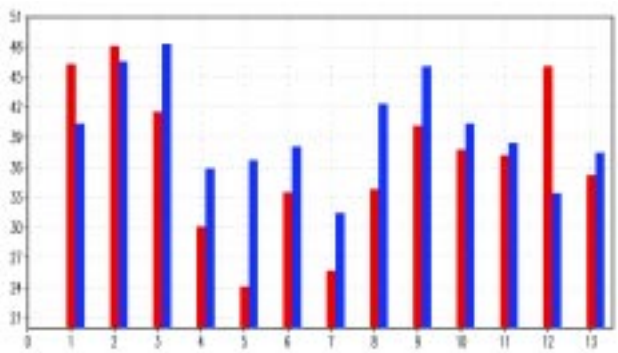

Figure 3.3. Bar chart of the percent variance explained by the leading components for the observation (red) and simulation (blue); months are numbered 1–12, with the annual data labelled as number 13.

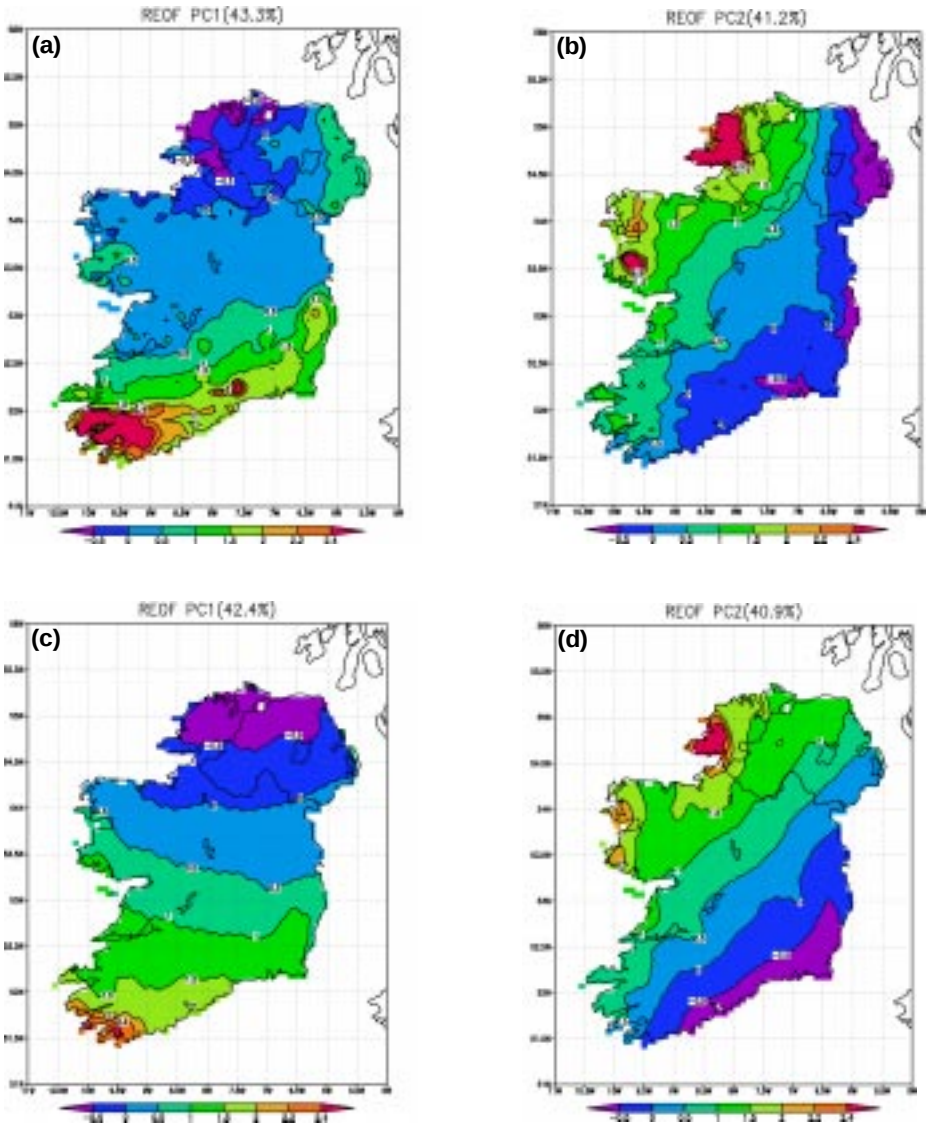

Figure 3.4. The first and second principal components of the observed (a, b) and simulated (c, d) precipitation for 1961–2000.

(Fig. 3.5b). Before 1975 it is still similar, while after 1975 the time series shows a stable increasing trend in the observation and simulation analysis.

Because the first two components (explaining more than 80% of the variance) show comparably low values for the time period before 1975, the precipitation is comparably low in this time period over the whole country. The increase in the average intensity, as well as in the variability of the first component with its precipitation maximum in the south-west after 1975, is consistent with Kiely's (1999) research. According to the second component, the precipitation shows a gradual increase in the west and north-west after 1975.

A more detailed analysis of the data shows that there are two major frequencies: one has a period of about 4 months, reflecting the seasonal variation, while the other has a period of about 1 year. Both frequencies are detectable in the observation and simulation data. Although the spatial patterns are different between the first and second components, the frequency analysis is similar. These two periods characterise quite well the evolution of precipitation over time.

3.5 Discussion and Conclusions

The annual and monthly precipitation analysis results show that the model can capture the leading spatial patterns in Ireland. However, the simulation tends to have

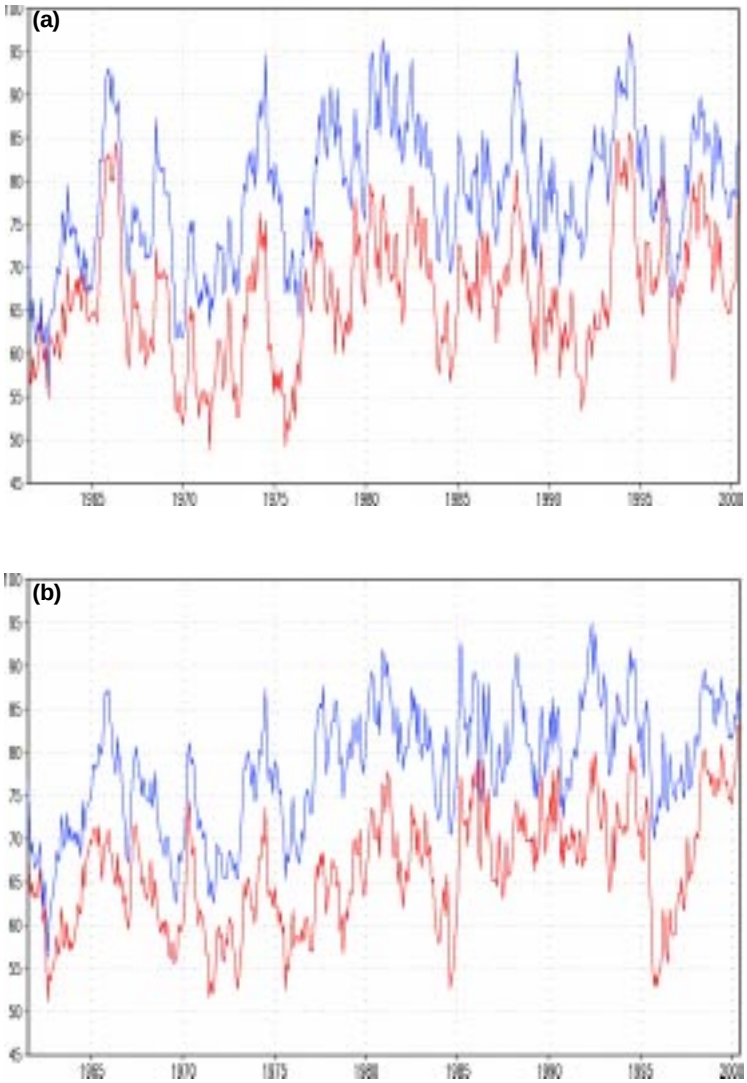

Figure 3.5. The first (a) and second (b) eigenvector of the observed (red) and simulated (blue) precipitation (one year moving average) in mm/month (1961–2000). The eigenvector reflects the time weighting given to the principal components shown in Fig. 3.4.

a less pronounced seasonal cycle compared to the observations. The transit from the wet winter to the dry summer season and from the dry to the wet season is slower in the model simulation. Summer-time precipitation amounts are overestimated in the simulation. Also, the orographically induced precipitation maxima are underestimated in the simulation.

The time evolution of the leading spatial patterns of the observed rainfall shows two major patterns. In one pattern, the precipitation maximum is located in the south-west of Ireland. The evolution of this pattern shows a strong decadal variability, which is very well simulated by the model. The time evolution of the second pattern, linked to precipitation maxima in the west and north-west of Ireland, shows a strong continuously increasing trend which is also well simulated by the model.

4 Simulation of the Future Climate: 2021–2060

Summary of contents: Projections for the future Irish climate were generated by downscaling the data from the German (Max Planck Institute) global model, ECHAM4, using a Regional Climate Model. Simulations were run for a reference period 1961–2000 and a future period 2021–2060; differences between the periods provide a measure of the expected climate change.

Results show a general warming in the future climate with mean monthly temperatures increasing typically between 1.25°C and 1.5°C. The largest increases are seen in the south-east and east, with the greatest warming occurring in July. For precipitation, the most significant changes occur in the months of June and December. June values show a decrease of about 10%, noticeably in the southern half of the country. March, July and August are largely unchanged but all other months show overall increases. December values show increases ranging between 10% in the south-east and 25% in the north-west. There is also some evidence of an increase in the frequency of extreme precipitation events (i.e. events of 20 mm or more per day) in the north-west.

4.1 Introduction

The UNFCCC provides the international structure for actions on anthropogenic climate change. The ultimate objective of the UNFCCC is stabilisation of atmospheric GHG concentrations at a level that would prevent dangerous anthropogenic interference with the climate system. The EU considered that a global temperature increase of more than 2°C above pre-industrial levels would inevitably result in dangerous climate change. To ensure that this level is not exceeded it is widely considered that stabilisation of atmospheric GHG levels at equivalent to between 450 and 550 ppm is required. Current atmospheric levels are just under 400 ppm.

The EU climate protection target has not been accepted by all Parties to the UNFCCC. This means that the extent of future action on climate change remains uncertain. Consequently, there is considerable uncertainty regarding the concentrations of GHG that are implicated in climate change. However, the social and political influences can be modelled on a general 'scenario' basis. For the same GHG scenario, there is considerable agreement between different simulations of the future climate up to about mid-century (see IPCC, 2001). This provides the justification for the premise used in this study. However, the results should be treated with some caution as they are based on the data from a single GCM. Ideally, we should downscale the data from several GCMs, using an 'ensemble' approach to quantify uncertainties. This study is a step along this path.

Simulation data from the Max Planck Institute ECHAM4/OPYC3 coupled atmosphere–ocean general circulation model (Roeckner *et al.,* 1996) were chosen to drive the RCM. This transient simulation, extending from 1860 to 2100, used observed GHG concentrations up to 1990 and the SRES-B2 scenario for the future (i.e. moderately increasing GHG concentrations; see Appendix IV and also refer to the UNEP GRID-ARENDAL web site http://www.grida.no/climate/ipcc/emission for further details). It is important to note that the GCM simulation was not linked to any meteorological observations in simulating the past climate; snapshots of the weather on particular days in the past will have little in common with the observed weather but averaged over seasons they should be in agreement. It is essential to generate a reference simulation, linked with the current and past climate, when downscaling with the RCM, to assess the future simulation. The reference run was chosen to cover the 40-year period 1961–2000[2] while the future run covered the period 2021–2060. Differences between the two runs give a measure of the expected change in the Irish climate.

Only the main results are presented here; further information can be found on the C4I web site http://www.c4i.ie.

4.2 Results

4.2.1 Mean sea level pressure (MSLP)

Figure 4.1 shows the MSLP field averaged over the 40-year integration period from 1961 to 2000. Differences between the RCM and ERA-40 data (Fig. 4.1c) show that the ECHAM4-driven model produces a slightly stronger gradient across Ireland, resulting in a stronger westerly airflow compared with the observation-based ERA-40 data.

2. 1961–1990 is the official WMO climate reference period. We use a longer period to aid comparison with the future period.

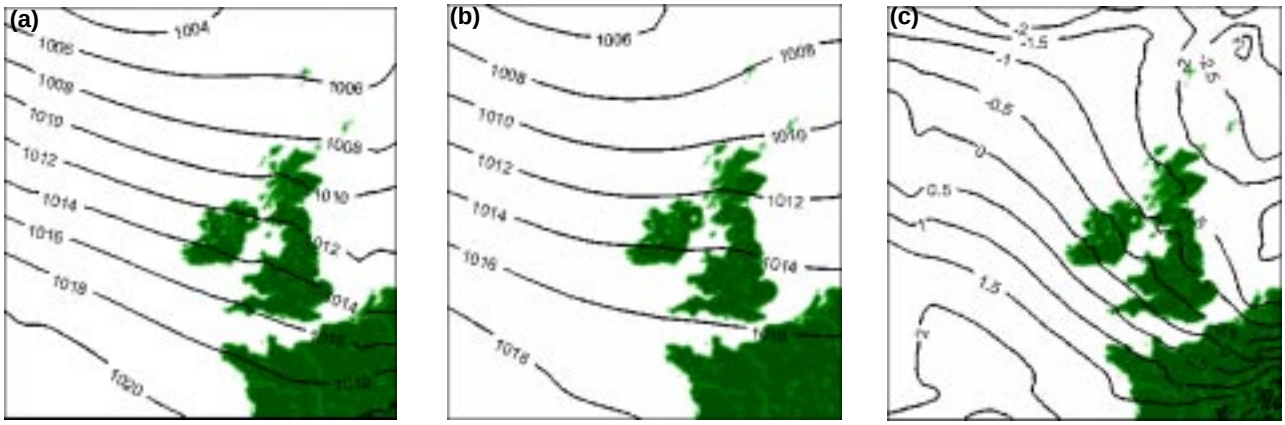

Figure 4.1. Average MSLP 1961–2000 (in hPa) from (a) the Regional Climate Model and (b) ERA-40 data. The mean difference field is shown in (c).

Plots of the mean differences between the reference (past) and future simulations are shown in Fig. 4.2. The differences are small but in the future period the mean pressure is slightly lower over the entire model domain – this is also reflected in the difference plot where all values are negative. The pressure gradient is slightly increased, particularly in the north of the model domain.

4.2.2 2-Metre temperature

Figure 4.3 shows the January and July average 2-m temperature over Ireland for 1961–2000 and differences relative to the observation-based UKCIP data set. In general, the data from the reference regional model run are too warm: January temperatures are about 1.5°C above observations and while the July data are in better agreement, there is still a warm bias in many areas. In addition, the annual variability is not as large as observed. However, the importance of the simulations is not in precisely reproducing the present climate, but rather in providing a reference data set for evaluating trends in the future climate.

Figure 4.4 compares the past (1961–2000) and future (2021–2060) ECHAM4-driven simulations. It can be seen that the average January temperatures over Ireland have increased between these two periods by about 1.25°C (Fig. 4.4b), with the largest increase in the south-east and east. The average July temperatures have increased even more, by about 1.5°C (Fig. 4.4d), again with the largest increase in the south and south-east.

The yearly 2-m temperature time series for Valentia is shown in Fig. 4.5. The reference simulation results (purple) show good inter-annual variability, but fail to reproduce the observed temperatures (blue) during the cooler 1980s. The change in temperatures between the reference and future simulation (shown in red) is clearly

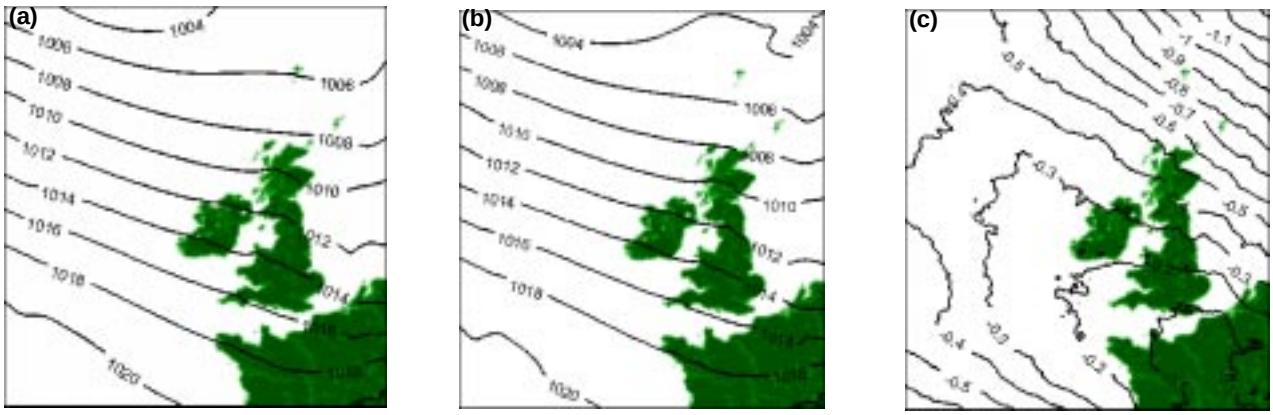

Figure 4.2. Average MSLP 1961–2000 (in hPa) from the ECHAM4-driven Regional Climate Model for (a) past/reference period (1961–2000) and (b) future period (2021–2060). Mean differences between the simulations are shown in (c).

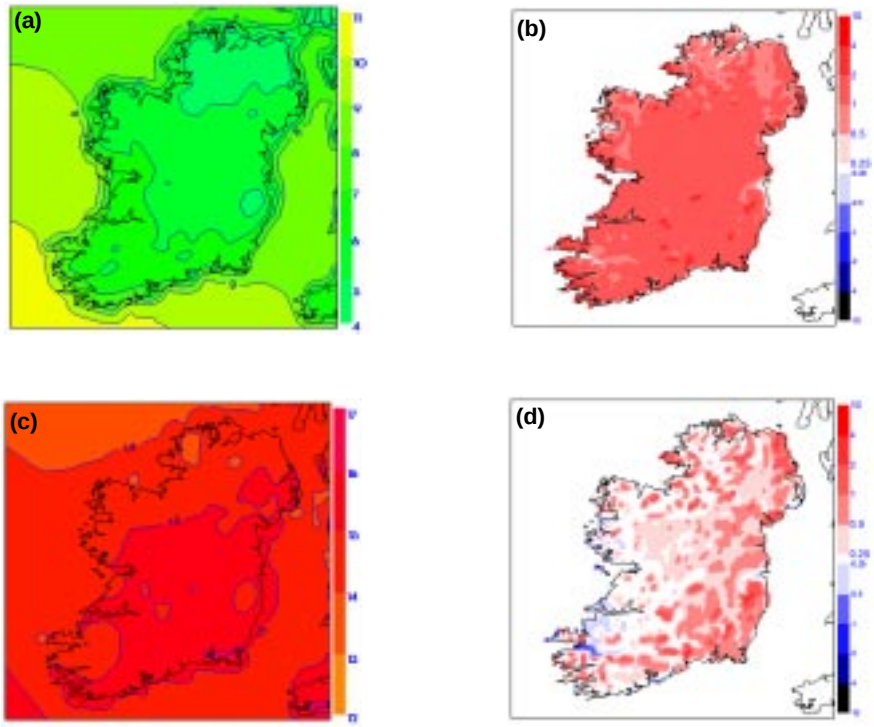

Figure 4.3. Regional Climate Model reference simulation driven by ECHAM4 data: average 2-m temperature (1961–2000) for (a) January and (c) July. Differences relative to the UKCIP observed data are shown in (b) and (d). Units: degrees Celsius.

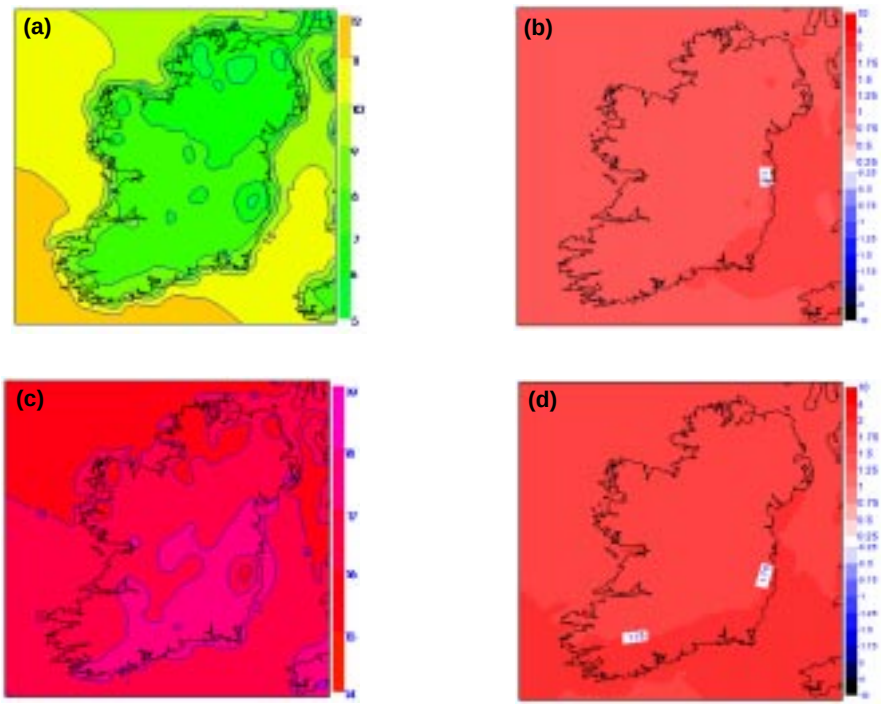

Figure 4.4. Regional Climate Model simulation for 2021–2060 driven by ECHAM4 data: average 2-m temperature for (a) January and (c) July. Differences relative to the reference (1961–2000) simulation are shown in (b) and (d). Units: degrees Celsius.

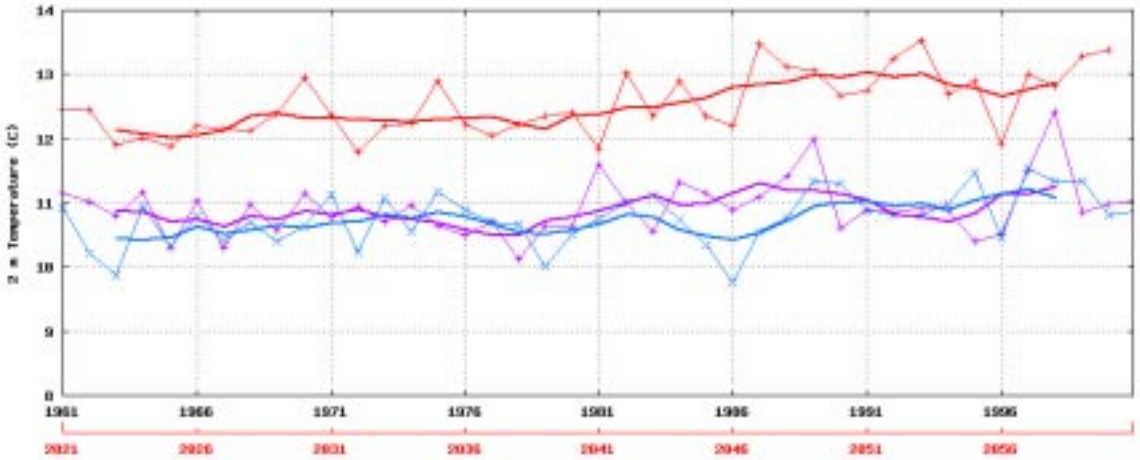

Figure 4.5. Yearly 2-m temperature time series for Valentia Observatory. Observed (blue), 1961–2000 reference simulation (purple), 2021–2060 future simulation (red); 5-year running average values are shown in bold.

visible, with an increase of about 1°C at the start of the future period rising to about 2°C by the 2050s. The inter-annual variability still exists, although almost all temperatures are warmer than those for the present climate.

4.2.3 Radiation and cloud cover

Figure 4.6 shows the yearly time series of the short-wave radiation at Valentia. The observations show a trend of decreasing short-wave radiation incident at the surface over the period 1961–2000. The reference simulation (1961–2000) produces more short-wave radiation than observed, and does not show any overall trend during the simulation period. Similarly, the future simulation data show no significant trend. Failure to capture the trend could be attributed to the fact that the ECHAM4 model has static aerosol concentrations; the 'global dimming' effect, which is probably linked to increasing concentrations of aerosols and a consequent reduction in radiation reaching the surface of the earth, is not taken into account.

Although there are no strong long-term trends in the simulated short-wave radiation at Valentia, there are some inter-annual differences that could be due to changes in cloud cover. Plots of the yearly mean cloud (Fig. 4.7) and relative changes between the reference and future RCM simulation data show some correlation with the short-wave radiation plots (Fig. 4.6).

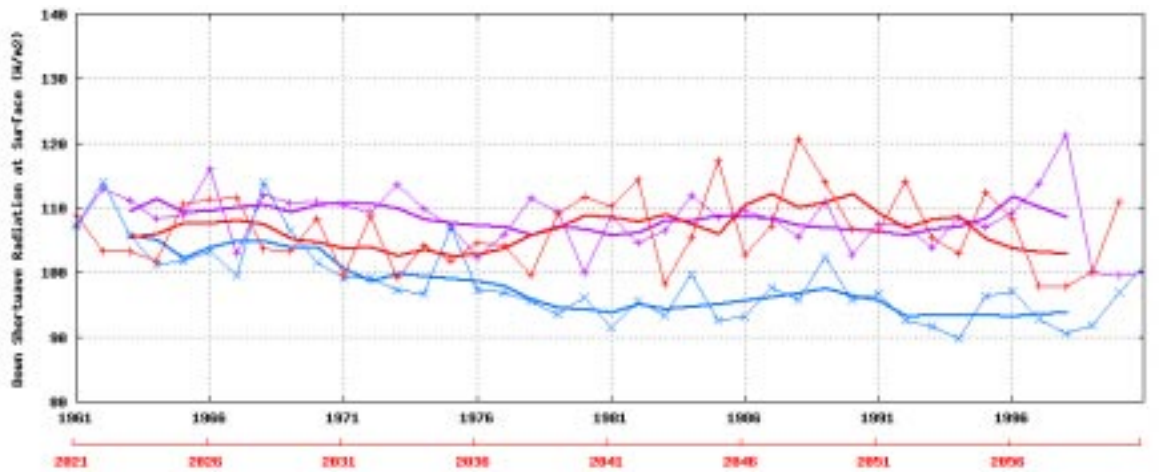

Figure 4.6. Yearly time series of short-wave radiation at Valentia Observatory. Observed (blue), 1961–2000 reference simulation (purple), 2021–2060 future simulation (red); 5-year running average values are shown in bold.

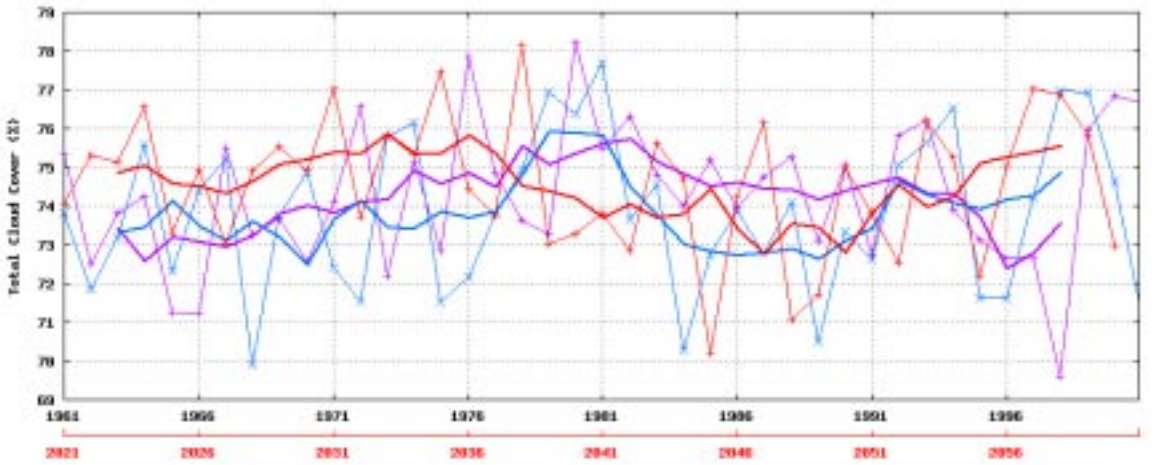

Figure 4.7. Yearly time series of cloud cover at Valentia Observatory. Observed (blue), 1961–2000 reference simulation (purple), 2021–2060 future simulation (red); 5-year running average values are shown in bold.

4.2.4 Precipitation

The months of June and December show the largest changes in average monthly precipitation between the reference and future simulations, as shown in Fig. 4.8. Over most of the southern half of the country, as well as in mountainous areas in the west and north, the June monthly rainfall amounts in the future simulation are over 10% lower than those in the 1961–2000 reference period. It is the only month which is significantly drier compared to the reference period. March, July and August are largely unchanged but all other months show overall increases in precipitation. December shows the largest increase with changes ranging from around 10% in the south-east to 25% in the north-west (Fig. 4.8d).

The yearly rainfall time series for Belmullet is shown in Figure 4.9. The reference simulation (purple) produces higher rainfall values than those observed (blue), showing that the ECHAM4 climate for the period 1961–2000 is too wet. The precipitation results for the future period (red) show an increase in rainfall amounts for most years compared to the reference simulation. With 5-year running average values the future simulation shows higher rainfall amounts for almost all years compared with the reference. The variability in the trend of the future precipitation is not as large as that for the reference, showing that higher annual rainfall amounts occur more consistently in the future than in the present climate.

The number of dry days per year (<0.2 mm) for Belmullet is shown in Fig. 4.10a. As in the case of the validation run (see Chapter 2), the model produces small amounts of rain too frequently, resulting in fewer dry days. Compared with the reference period the number of dry days in the future simulation is similar.

The frequency of heavy precipitation (>20 mm) days per year is shown for Belmullet in Fig. 4.10b. For the reference period, the model over-predicts the frequency of such events. This is quite likely related to the more pronounced westerly flow in the ECHAM4 data which may give rise to a moister atmosphere with increased precipitation. The average number of heavy rainfall days seems to have increased in the future simulation results although both periods remain within the range of 4 to 26 days per year.

4.2.5 10-Metre wind

Detailed results for the ECHAM4 simulations are available on the C4I web site http://www.c4i.ie.

4.3 Conclusions

Projections for the future Irish climate have been generated using the RCM. Simulations were run for a reference period 1961–2000 and a future period 2021–2060; differences between the periods provide a measure of expected climate change.

Results show a general warming in the future climate with mean monthly temperatures increasing typically between 1.25°C and 1.5°C. The largest increases are seen in the south-east and east, with the greatest warming occurring in July. For precipitation, the most significant changes occur in the months of June and December. June values

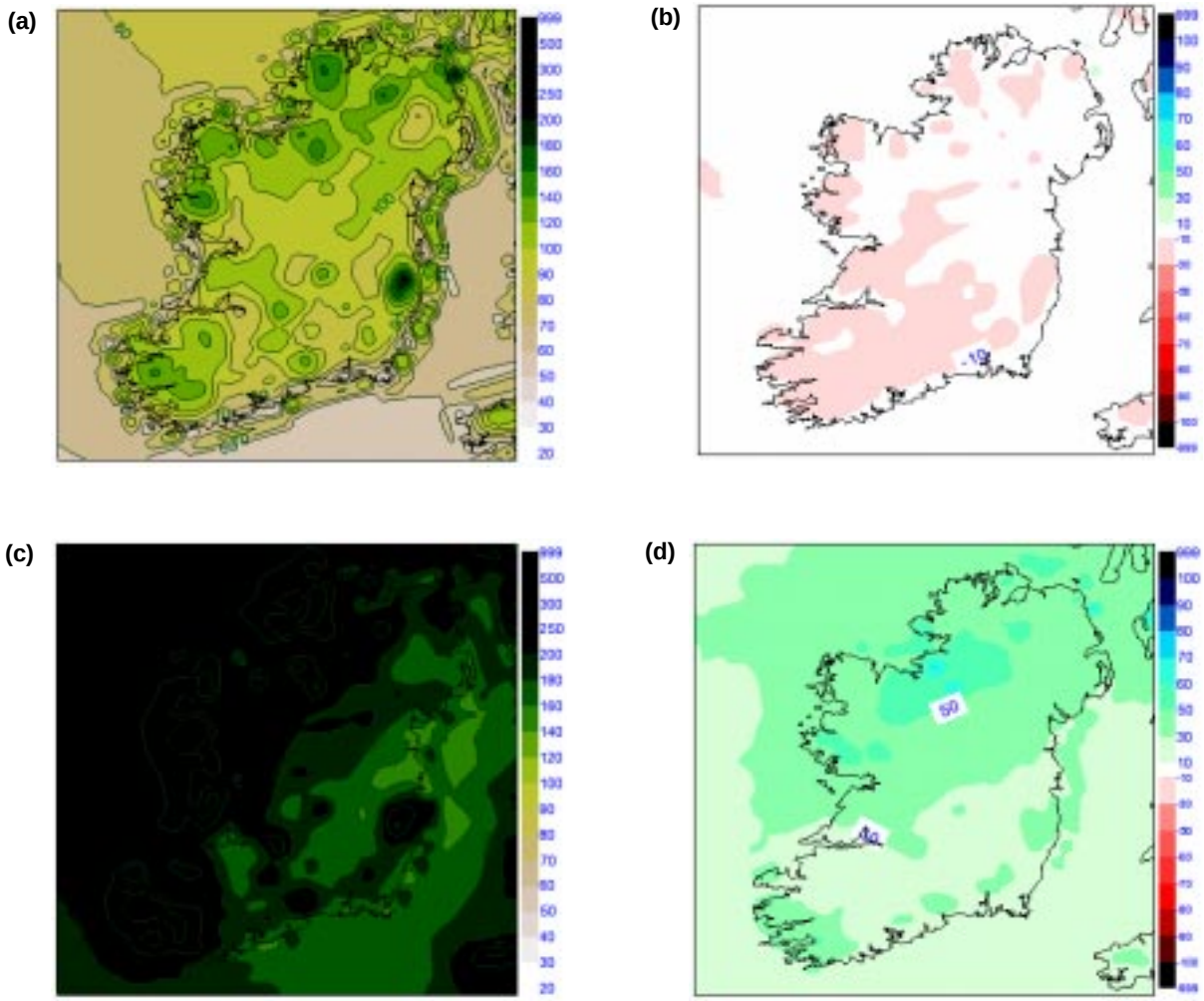

Figure 4.8. Regional Climate Model simulation for 2021–2060 driven by ECHAM4 data: monthly rainfall accumulation for (a) June and (c) December. Differences relative to the reference (1961–2000) simulation are shown in (b) and (d). Units: millimetres.

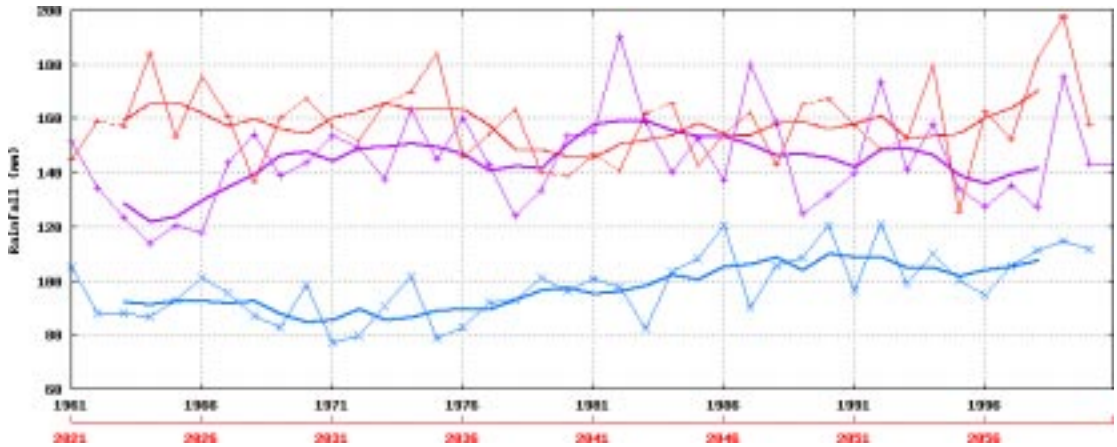

Figure 4.9. Yearly rainfall time series for Belmullet. Observed (blue), 1961–2000 reference simulation (purple), 2021–2060 future simulation (red); 5-year running average values are shown in bold.

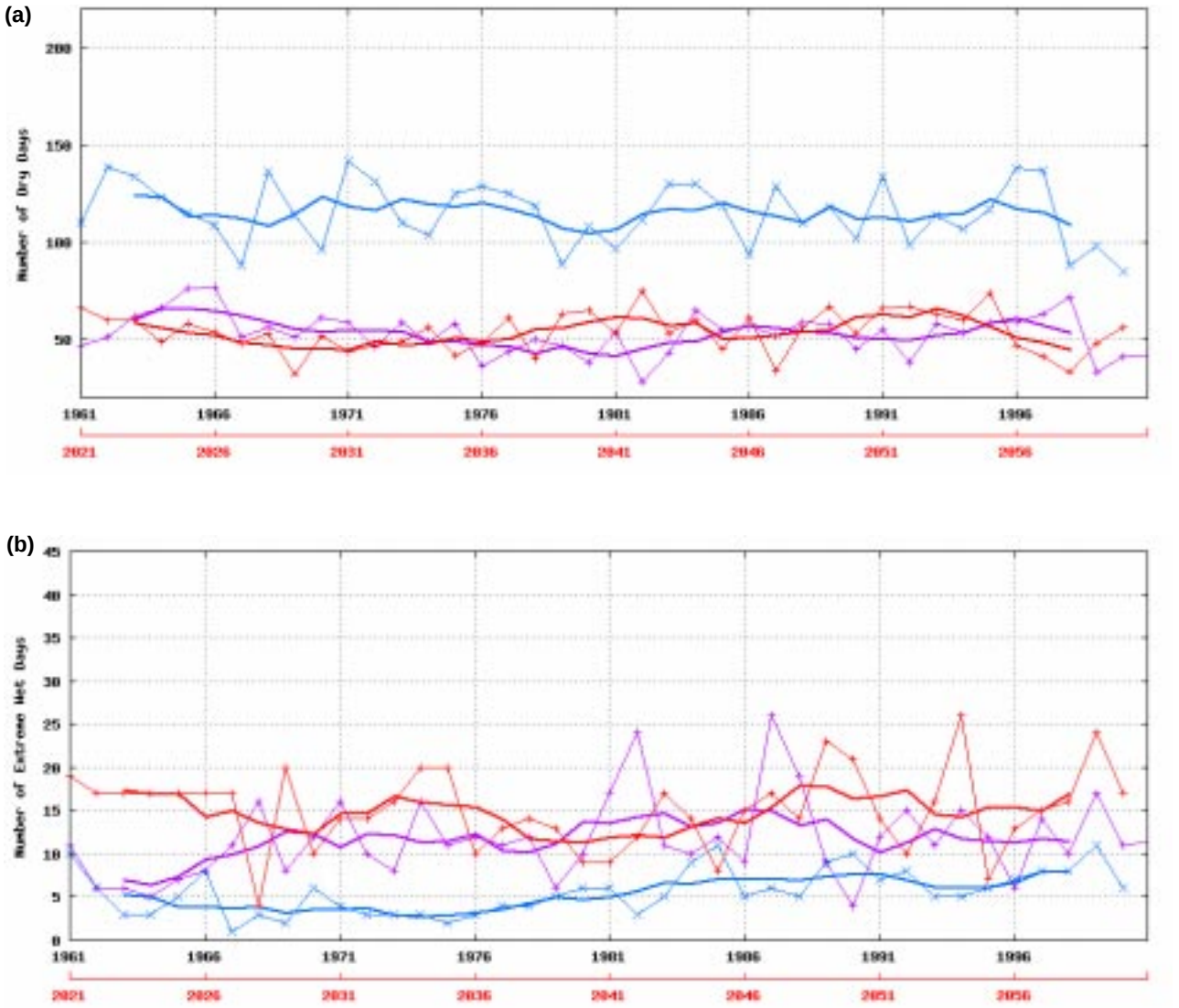

Figure 4.10. Yearly time series for Belmullet: (a) number of dry days (<0.2 mm), (b) number of heavy rainfall days (>20.0 mm). Observed (blue), 1961–2000 reference simulation (purple), 2021–2060 future simulation (red); 5-year running average values are shown in bold.

show a decrease of about 10%, noticeably in the southern half of the country. March, July and August are largely unchanged but all other months show overall increases. December values show increases ranging between 10% in the south-east and 25% in the north-west. There is also some evidence of an increase in the frequency of extreme precipitation events (20 mm or more per day) in the north-west. For cloud cover and short-wave radiation, the signals are more mixed with no obvious trends in the future. However, the results need to be treated cautiously as the ECHAM4 general circulation model has a static aerosol representation and the regional model does not capture the decreasing trend in short-wave radiation, possibly linked to increasing aerosol concentrations, seen in the observational records from stations such as Valentia.

5 The Impact of Climate Change on River Flooding under Different Climate Scenarios

Summary of contents: Application of a standard hydrological model to the Suir catchment area shows that the model is capable of capturing the variability of river discharge with reasonable accuracy when driven by observations (calibration) or high-resolution data from a Regional Climate Model (validation).

When driven by the projected precipitation data from the RCM for the period 2021–2060, the hydrological model shows a significant increase in the more intense discharge episodes, and an increase in the frequency of extreme discharges.

5.1 Introduction

The IPCC has stated that mean surface temperatures may rise 0.3–0.6°C per decade in the 21st century (IPCC, 2001). As increased temperatures will lead to greater amounts of water vapour in the atmosphere and an accelerated global water cycle, it is reasonable to expect that river catchment areas will be exposed to a greater risk of flooding. Many impact studies have already been carried out to assess such risks in other countries (Bergstrom *et al.*, 2001; Pilling and Jones, 2002; Arnel, 2003). This study examines the risks for Ireland using the Suir catchment area as a test case.

The Land Surface Parameterisation (LSP) scheme is an important part of the RCM; it acts as a bridge connecting the atmosphere and water cycle. Significant efforts have been made to improve the representation of the land surface–atmosphere interaction during the last two decades, particularly for the hydrological component. However, because of the different spatial resolutions of the climate and hydrological models, it is still difficult to couple the models directly. For the hydrological model, the most important processes in the context of climate change and river flooding are known to be precipitation and evapotranspiration. In this study, the precipitation values from different RCM simulations are used to drive the hydrological model in the Suir catchment area. For evapotranspiration data, the monthly mean climate values from Johnstown Castle are used as proxies in the catchment area.

5.1.1 The HBV hydrological model

The hydrological discharge model (HBV) of the SMHI is used in this study (Bergstrom, 1995; Lindstrom *et al.*, 1997). The model is a semi-distributed, conceptual hydrological model using sub-basins as the primary hydrological units; it takes into account area-elevation distribution and basic land-use categories (forest, open areas and lakes). The sub-basins option is used in geographically or climatologically heterogeneous basins or large lakes. It has been widely used in Europe and other parts of the world in applications such as hydrological forecasting, water balance mapping and climate change studies.

5.1.2 Data sets

To investigate the influence of climate change on regional water resources and flooding, three global data sets were used to drive the RCM. For the past climate (1961–2000), ERA-40 and ECHAM4 data were used, while for the future climate simulation (2021–2060) the model was driven by ECHAM4 data consistent with the SRES-B2 scenario (see Appendix IV for details). As the ERA-40 data are based on observations and are generally regarded as providing an accurate description of the atmosphere, they provide an excellent means for testing the performance of the climate model in a hydrological application. To consider the effect of the different boundary data on the future climate simulation run, the ECHAM4 past climate simulation was used as a control.

5.2 Results

5.2.1 Calibration

In the HBV model, the parameters with the largest uncertainty are related to the soil moisture parameterisation scheme. The main parameters are FC (maximum soil moisture storage in millimetres), LP (fraction of FC above which potential evapotranspiration occurs and below which evapotranspiration will be reduced) and the coefficient BETA (determining the relative contribution to run-off from a millimetre of precipitation at a given soil moisture deficit). These parameters are dependent on the properties of the catchment, such as the land-use type, the wilting point and soil porosity. Because of the uncertainty, the Monte Carlo Random Sampling (MCRS) method is popularly

used for the parameter estimation. However, as the HBV program source code is not available, the above method is difficult to apply. In order to overcome this obstacle, quasi-stratified sampling in the form of Latin Hypercube Sampling (McKay *et al.*, 1979) was used. In this method, the limited sampling numbers can produce similar results to the Monte Carlo approach (Yu *et al.*, 2001).

For the calibration of the Suir catchment run, observed precipitation data for the period January 1960 to December 1964 and monthly mean climate evapotranspiration data were used to drive the HBV model. The actual catchment area and rainfall stations are shown in Fig. 5.1. Note that the calibration period includes relatively dry and wet years. Although insufficient observation data coverage limited the duration of the calibration to 5 years, it should be sufficient according to the model documentation of SMHI, which recommends the use of 5–10 years of data. The performance of the model was judged using a modified R^2 statistical correlation measure, defined as follows.

$$R^2 = \frac{(\Sigma(QR - QR_{mean})^2 - \Sigma(QC - QR)^2)}{\Sigma(QR - QR_{mean})^2}$$

where QC represents computed discharge, QR is observed discharge and QR_{mean} is the mean of QR over the calibration period.

For the calibration of Suir catchment data, the R^2 value (unity for perfect performance) was 0.787.

Figure 5.2 presents the calibration results. Except for the peak values, which are slightly underestimated, the variation in the simulated discharge coincides with the observed discharge fairly well.

5.2.2 Validation

In the validation run, the parameter values are kept the same as in the calibration, but simulations are repeated with independent input series from different present-day simulation results. Results are shown in Fig. 5.3. The evolution of the simulated discharge shows good agreement with observed data, similar to the calibration run and with peak values underestimated. On the whole, the simulation is a little worse compared to the calibration run with an R^2 value of only 0.545, while the correlation coefficient reaches 0.79. This confirms that the model simulates the evolution of the discharge well, whereas the underestimated peak values caused the R^2 value to be relatively low. Figure 5.4 shows the return values of the annual extremes of the observation and ERA-40-driven simulation. The distribution of return values for the different return periods show good agreement, although they are systematically underestimated by 15–20% in the simulation.

5.2.3 Future

Figure 5.5 shows the impact of climate change on the river discharge. For the past climate, the ECHAM4-driven

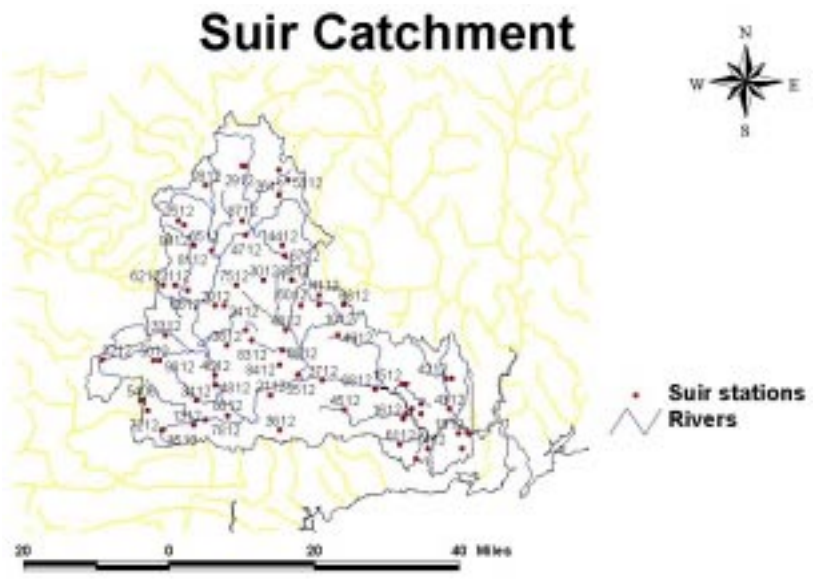

Figure 5.1. Suir catchment area and rainfall stations.

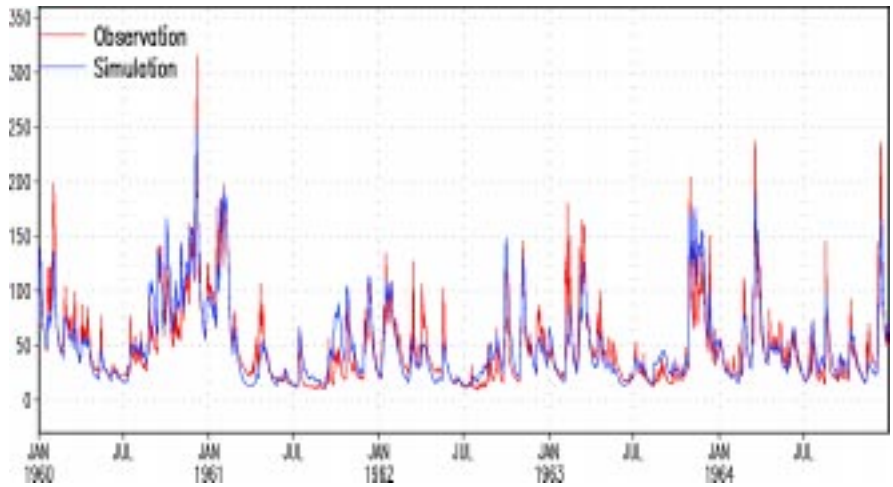

Figure 5.2. Observed and simulated (using observed precipitation data to drive the HBV model) discharge (m^3/s).

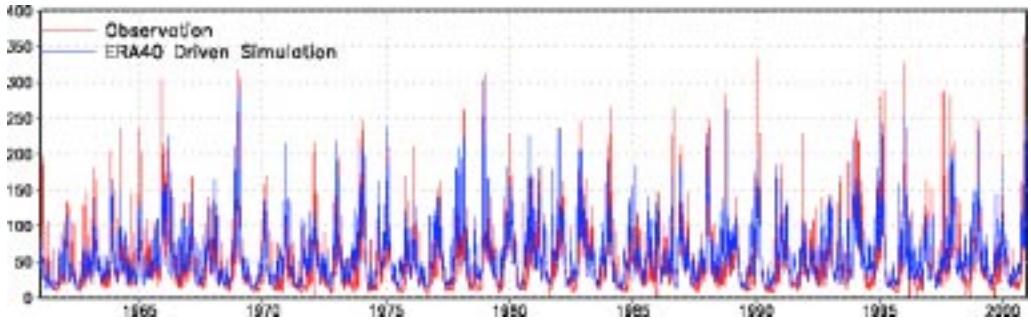

Figure 5.3. Observed and simulated (ERA-40-driven simulation) discharge (m^3/s).

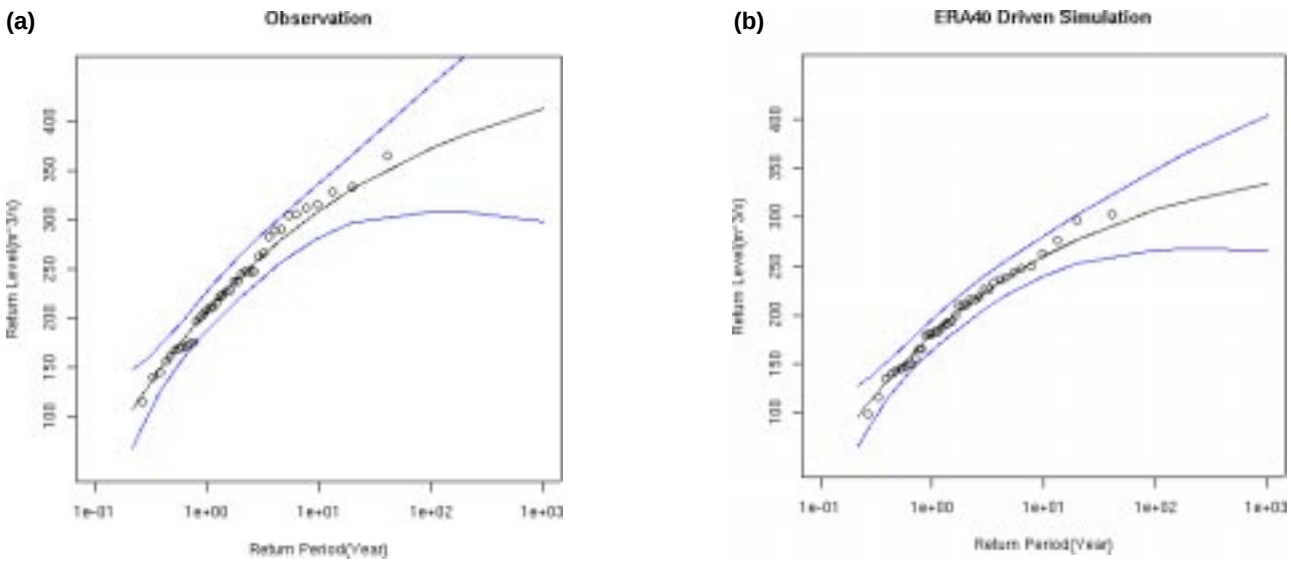

Figure 5.4. Return values of observed (a) and simulated (ERA-40-driven simulation) (b) maximum annual discharge.

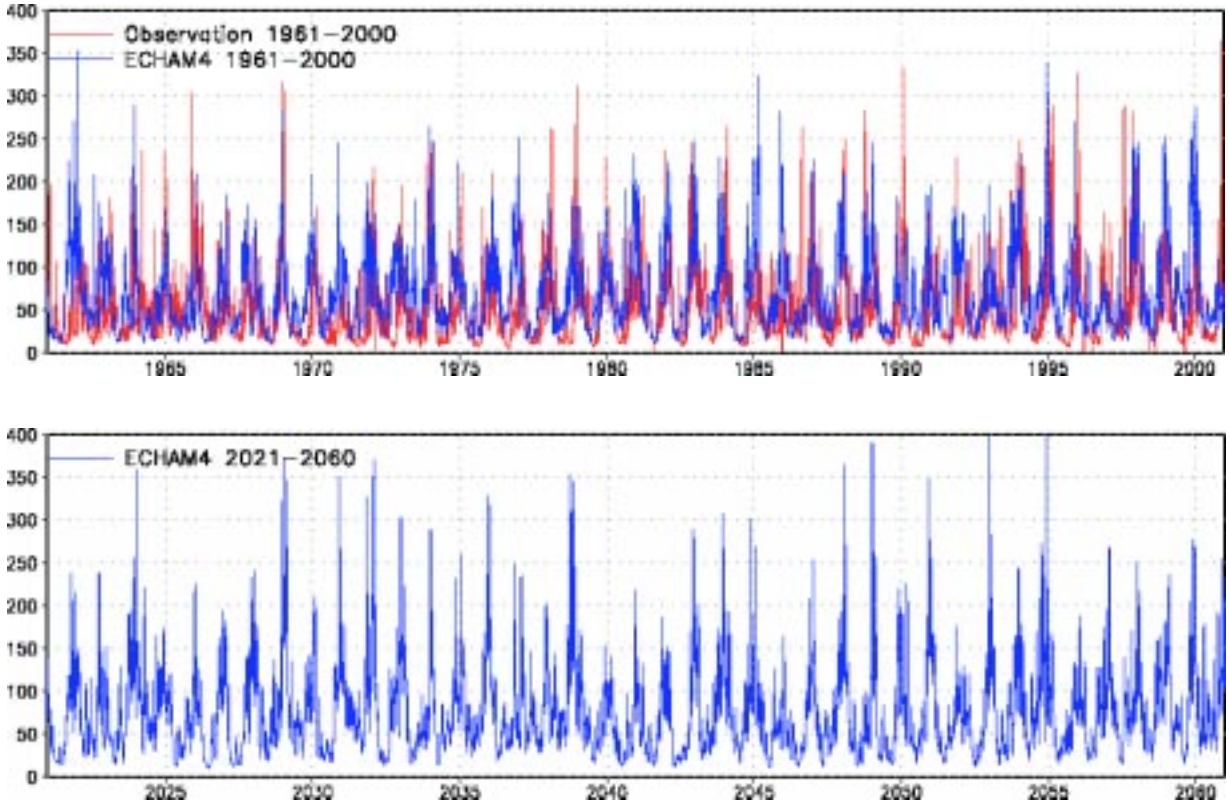

Figure 5.5. Simulated discharge using the ECHAM4-driven Regional Climate Model simulation for the past and future climate and observed discharge (m^3/s).

control simulation slightly over-predicts the discharge compared to the observations (Fig. 5.5a), and the timing of peak events is slightly shifted. Note, however, that we cannot expect an exact agreement concerning the timing of peak events between observation and simulation as the ECHAM4 data are based on averaged atmospheric conditions. However, the number of peak values is similar, which gives us confidence in the future projections. In the future run (Fig. 5.5b), the frequency and intensity of heavy discharges (e.g. >350 m^3/s) have clearly increased compared to the control run (Fig. 5.5a). The return value analysis (Fig. 5.6) also shows similar results with the 10-year return value increasing from about 290 to 360 m^3/s. Figure 5.7 shows the effect of climate change on the

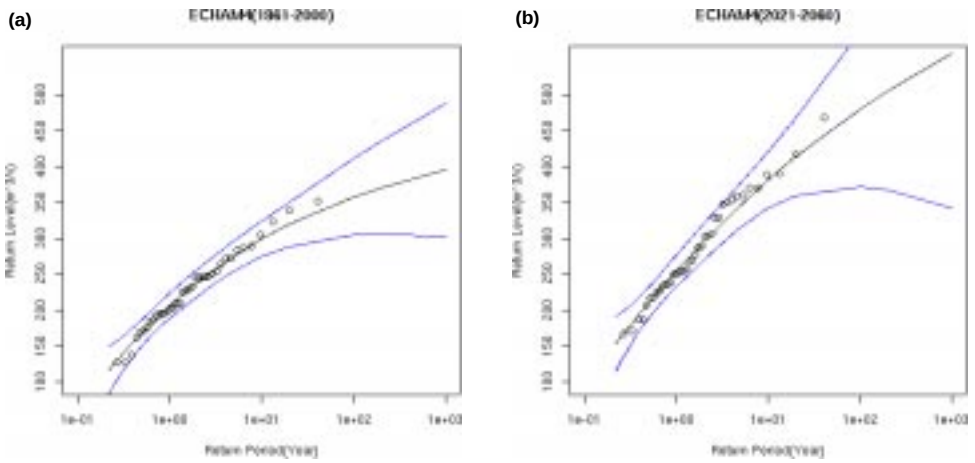

Figure 5.6. Return values of maximum annual discharge using the ECHAM4-driven Regional Climate Model simulation for (a) present-day climate (1961-2000) and (b) future climate (2021-2060).

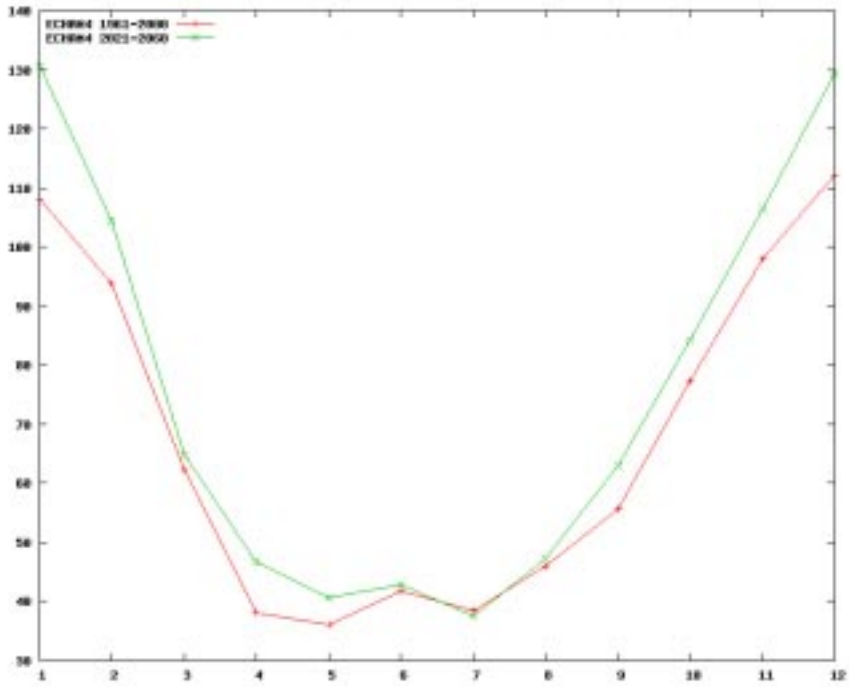

Figure 5.7. Annual cycle of simulated discharge driven by ECHAM4 data for the past (red) and future (green) climate (m^3/s).

annual cycle of the discharge: it remains unchanged in the dry season, but increases by up to 20% in December and January.

5.3 Conclusions

Application of the HBV model to the Suir catchment area shows that the hydrological model is capable of capturing the local variability of river discharge with reasonable accuracy when driven by observations (calibration) or the output from an RCM driven by high resolution re-analysis data (validation). In both cases, the same model parameters were used in the HBV model.

Using the simulation data from the RCM for the future period (2021–2060), the hydrological model shows a significant increase in the more intense discharge episodes, a pattern that is also shown in the return values of extreme discharge. This has implications for future planning to reduce impacts of flooding.

6 Cyclone Statistics and Tracks in the Climate Simulations: Past and Future

Summary of contents: To assess the ability of the Regional Climate Model to realistically reproduce the frequency and intensity of cyclones, data from the RCM simulation (1961–2000) driven by standard re-analysis meteorological data, were compared against the re-analysis data, using an algorithm developed to identify and track cyclones. Analysis of the frequency and intensity of cyclones shows that the RCM is in good agreement with the re-analysis data. The number of weak cyclones/storms with core pressures between 990 and 1000 hPa is overestimated by 20 to 30% but the number of intense cyclones/storms with core pressures of less than 950 hPa is very well captured.

For the future period, climate data from the ECHAM4-driven RCM simulation were used (based on the SRES-B2 emission scenario of GHG concentrations). Results for the reference (1961–2000) and the future (2021–2060) simulations were compared. The total number of cyclones with core pressure less than 1000 hPa and their seasonal and spatial distributions are similar for both periods. The frequency of very intense cyclones/storms with core pressures less than 950 hPa shows substantial changes: a 15% increase in the future simulation with even stronger increases in winter and spring seasons. Only the autumn numbers show a decrease in these systems. The tracks of these storms are also displaced further south relative to those in the reference simulation.

6.1 Introduction

The damage and disruption caused by intense low-pressure cyclones or storms can cause significant hardship for ecosystems and normal socio–economic activities, particularly in transport, energy and agriculture. This is most evident in tropical and subtropical regions which are impacted by hurricane systems. There are considerable ongoing efforts to improve the prediction of the intensity and movement of such storms, which even outside of the hurricane zones can be very damaging and economically costly. Understanding the impacts of projected changes in such systems as a result of climate change is an important task in predicting impacts. Here, analyses of projected changes in these areas are presented.

6.1.1 Tracking cyclones

The following algorithm was used to track the movement of cyclones.

On a horizontal grid of $N_x \times N_y$ points a low-pressure centre is identified at grid point *(i, j)* if these criteria are met:

- the pressure value, $p(i, j)$, is less than a given threshold, e.g. 1000 hPa;
- the point is a local minimum of pressure.

A point *(i, j)* is defined to be a local minimum of surface pressure if its pressure value $p(i, j)$ is less than the pressure values of all points contained in the surrounding four grid boxes (i.e. the surrounding 80 grid points, see Fig. 6.1). This corresponds to $p(i, j)$ being the minimum pressure within a distance of approximately 53 km in all directions. Since for each point we examine the four surrounding grid boxes, we do not take into account the boundary points and the three nearest points to the boundaries.

For example, a point will be identified as the centre of a cyclone if for the pressure value $p(i, j)$, we have:

$$p(i, j) < 1000 \text{ hPa}$$

and

$$p(i, j) < p(i + k, j + l),\ k = -4,\ldots..,+4\ (k \neq 0)$$

where

$$4 < i < N_x - 3 \text{ and } 4 < j < N_y - 3.$$

6.1.2 Cyclone statistics

The algorithm was applied to the RCM results and the ERA-40 re-analysis data. As the ERA-40 data are only available at 6-h intervals, the same interval was used for the RCM data. Figure 6.2a shows the frequency of lows as a function of core-pressure value for both data sets. The data bins along the x-axis have an increment of 1 hPa.

Although both curves in Fig. 6.2a follow a similar trend, the RCM returns substantially more lows, particularly at higher pressure values. The discrepancy arises from the fact that the RCM tends to split a large-scale low-pressure system with only one local minimum in the ERA-40 data

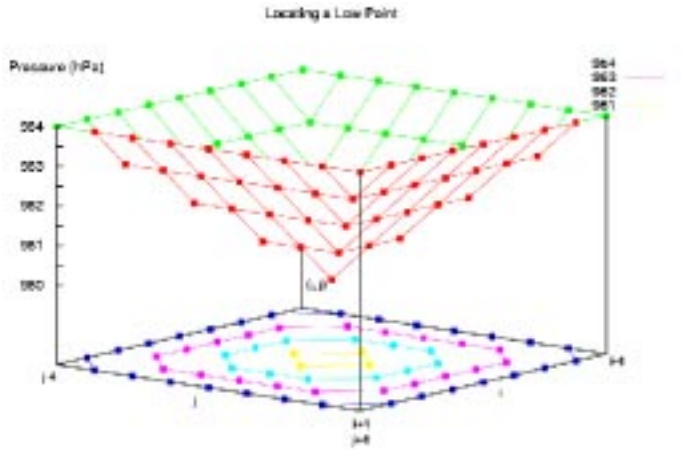

Figure 6.1. Locating a low point.

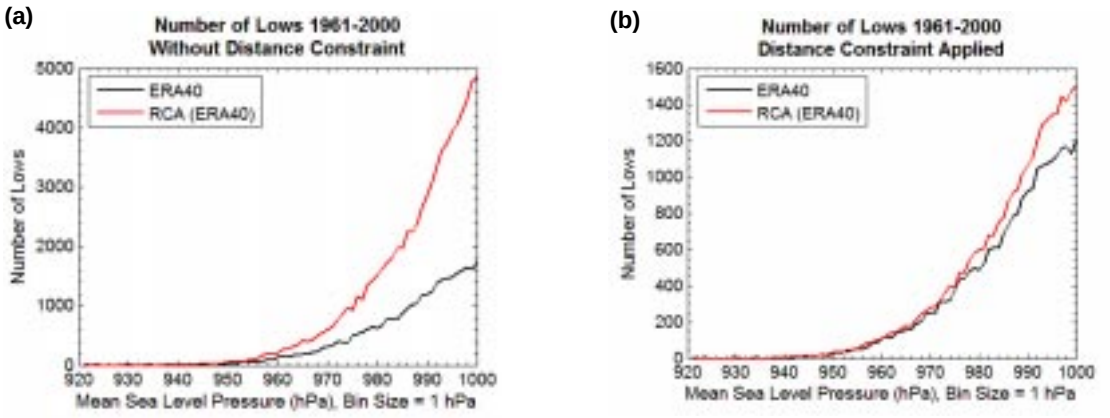

Figure 6.2. Frequency of lows as a function of core pressure (a) without using a distance constraint, and (b) using a distant constraint. Frequency is shown for the ERA-40 re-analysis data (black) and the Regional Climate Model driven by the re-analysis data (red).

into several local minima that are counted as separate lows in our algorithm (Fig. 6.3). This is a common occurrence in RCM simulations and since the local minima obviously belong to the same system we introduce an extra constraint in the algorithm: two local minima are considered to belong to the same system if they are less than 1000 km apart. The distance of 1000 km was chosen since this is a typical extension of a low-pressure system. With this constraint the low-pressure system is assigned the minimum pressure value and its position is taken to be the position of this minimum. The revised statistics (Fig. 6.2b) show much better agreement with ERA-40.

Figure 6.4a shows the annual number of lows with a core pressure of less than 1000 hPa. The patterns are very similar for the RCM and ERA-40 data with the model numbers being slightly higher. This is also reflected in the ratio plot shown in Fig. 6.4b.

The seasonal number of lows over the 40-year period is depicted in Fig. 6.4c. Both the RCM and the ERA-40 data follow the same trend with the greatest and lowest number of systems occurring in winter and summer, respectively. Figure 6.4d shows the spatial distribution of the cyclones split into quadrants. The percentages are broadly similar but the regional model has slightly more lows in the eastern half of the area compared with ERA-40. As expected, most of the lows fall into the northern half of the area.

The time-series plot of the number of lows (Fig. 6.5) shows that the RCM is capable of capturing the seasonal variations.

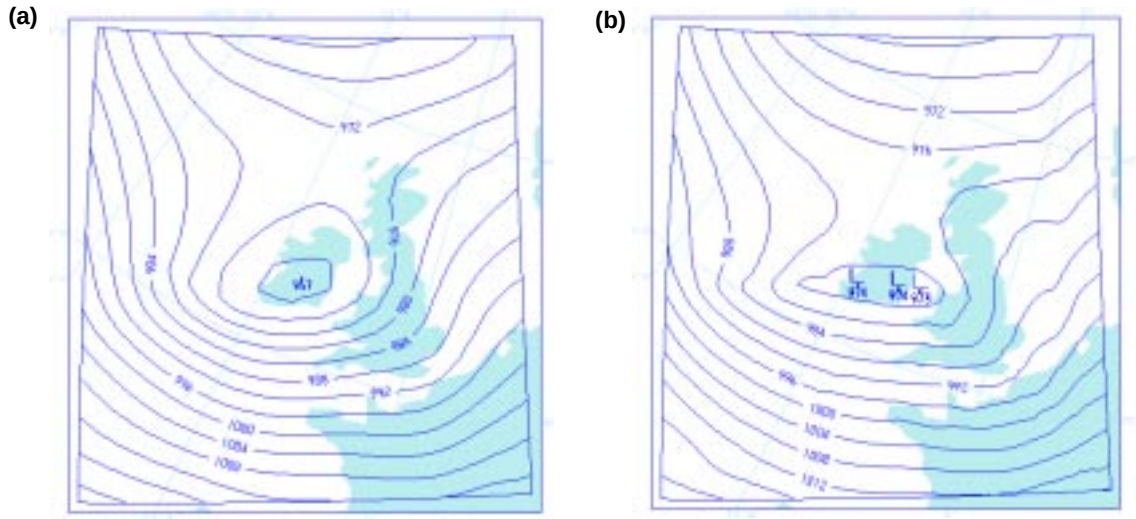

Figure 6.3. An example of (a) one local minimum in ERA-40 and (b) three local minima in the Regional Climate Model.

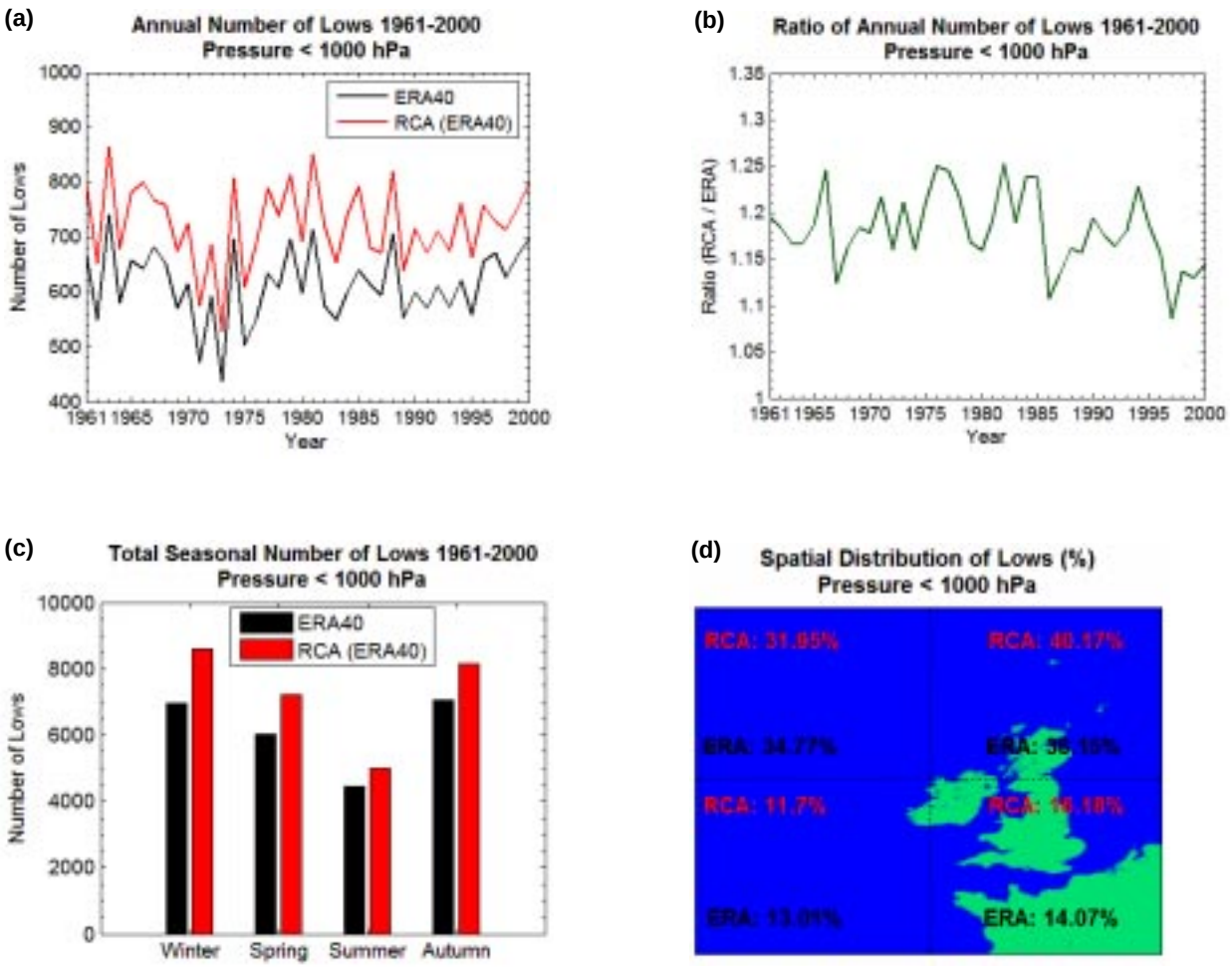

Figure 6.4. (a) ERA-40 and Regional Climate Model annual number of lows, (b) ratio of annual number of lows (RCM/ERA-40), (c) total seasonal number of lows, and (d) spatial distribution of lows with a core pressure of less than 1000 hPa in the regional model and ERA-40 for the time period 1961–2000.

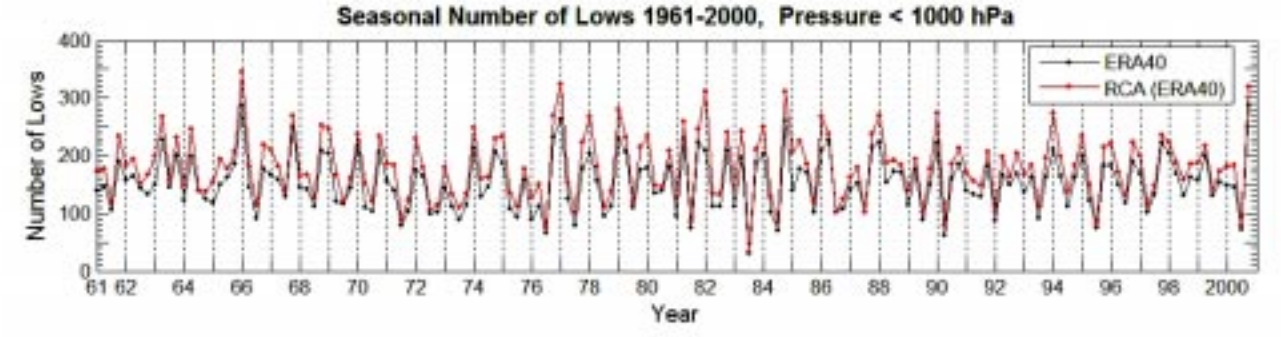

Figure 6.5. Seasonal number of lows with a core pressure of less than 1000 hPa from ERA-40 and the Regional Climate Model for 1961–2000.

6.1.3 Intense cyclones

In this section, statistics are presented for cyclones with core pressures less than 950 hPa. Note that with the lower pressure threshold the RCM results agree more closely with the ERA-40 re-analysis data. This is evident from the plot depicting the annual number of lows (Fig. 6.6a). The seasonal and spatial distributions of the cyclones are shown in Figs 6.6b and 6.6c, respectively. As expected, most of the intense cyclones occur in winter and are located in the northern half of the area. A time-series plot of the seasonal number of lows (Fig. 6.7) shows good agreement between the RCM and ERA-40. Note the increase in frequency in the 1990s.

It is encouraging that the results compare well for intense cyclones not only in the annual numbers, but also in the spatial and seasonal distributions, since extreme events are interesting in terms of impacts.

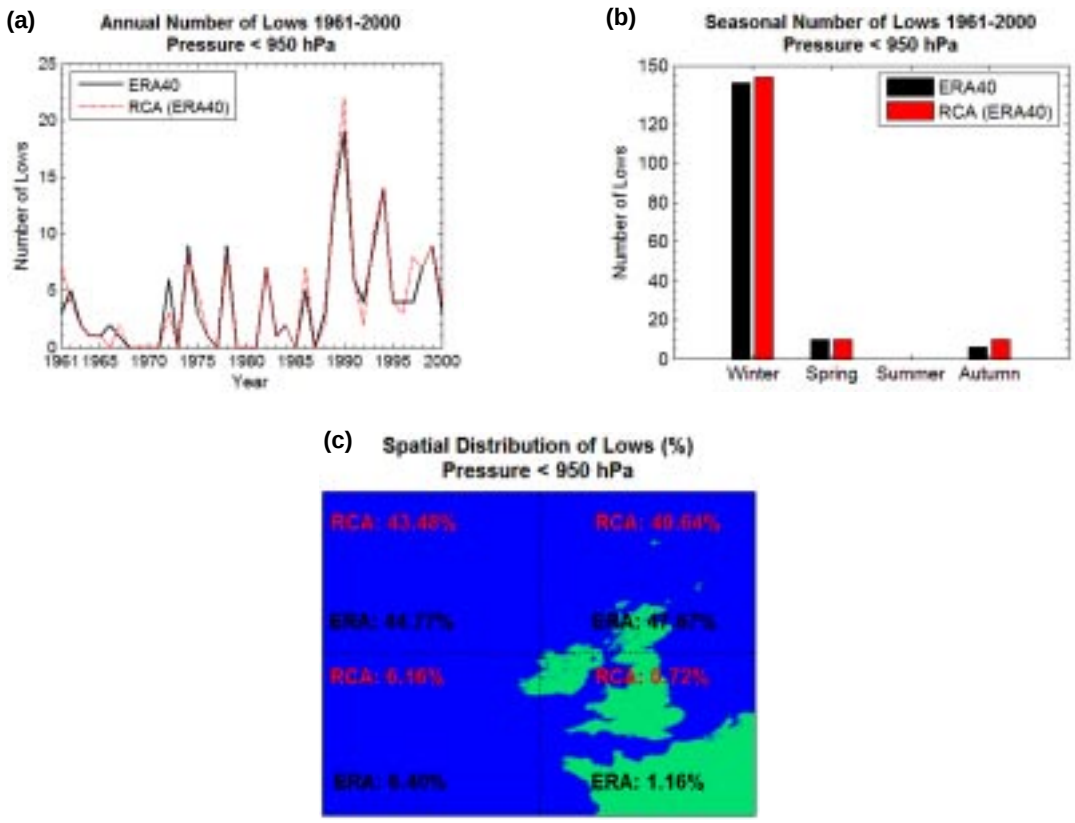

Figure 6.6. (a) Annual, (b) seasonal and (c) spatial distribution of the number of lows with a core pressure of less than 950 hPa in ERA-40 and the Regional Climate Model.

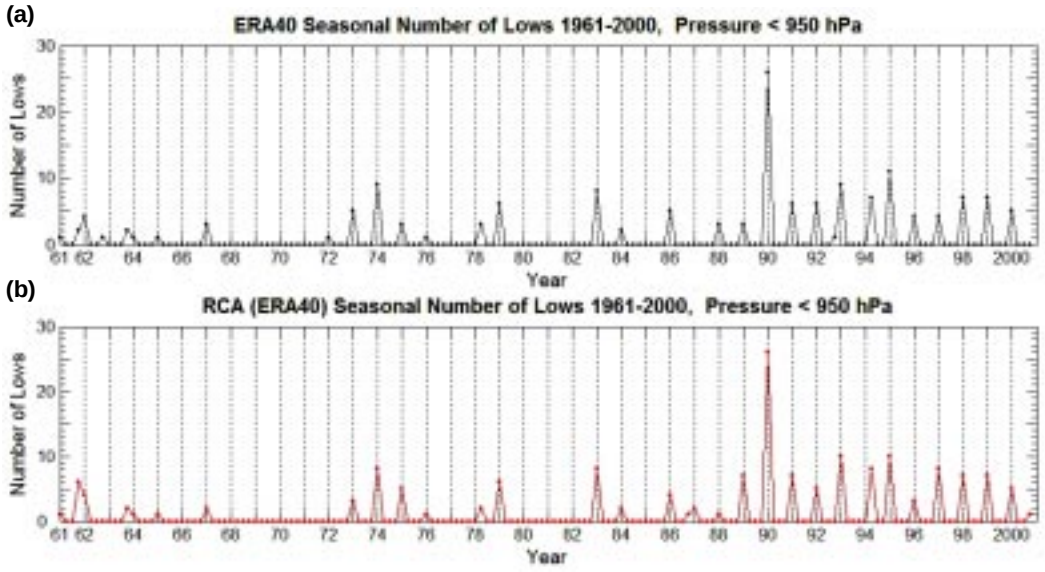

Figure 6.7. Seasonal number of lows with a core pressure of less than 950 hPa from ERA-40 (top) and the Regional Climate Model (bottom) for 1961–2000.

6.2 Cyclone Tracking

In this section, the spatial movement of cyclones with a core pressure less than 950 hPa is examined. To track the movement of the systems the cyclone centres are located at output times t and $t + \Delta$, where Δ is the data output frequency, set to 6 h to suit the ERA-40 data. A cyclone at time t is considered to be the same cyclone identified at time $t + \Delta$ if the estimated speed of movement, based on the great circle distance between the positions, is less than 120 km/h. In addition, only cyclones that exist for at least 24 h are considered.

Applied to the RCM and ERA-40 fields (Fig. 6.8) we can see that the RCM is in good agreement with ERA-40.

Results for one particular storm that caused widespread damage when it crossed Ireland and the UK on 25 January 1990 are shown in Fig. 6.9. The RCM track of this so-called Burns' Day storm, while a little too far south, agrees well with the ERA-40 track. However, the intensification of the system lags ERA-40 although it does eventually catch up with an extreme pressure of 950 hPa (Fig 6.10).

6.3 Simulation of the Future Climate

This section examines the impact of climate change on the frequency and intensity of cyclones, using the two ECHAM4-driven RCM simulations for 1961–2000 (reference simulation) and 2021–2060 (future simulation) described in Chapter 4. Data at 3-h intervals were used.

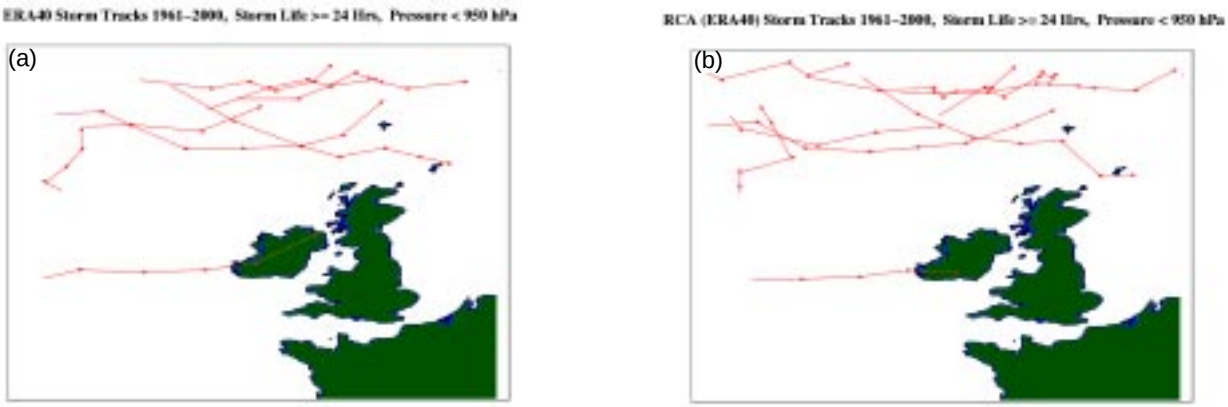

Figure 6.8. Tracks of storms with a core pressure of less than 950 hPa and with a lifetime of at least 24 h from (a) ERA-40 and (b) the Regional Climate Model for the time period 1961–2000.

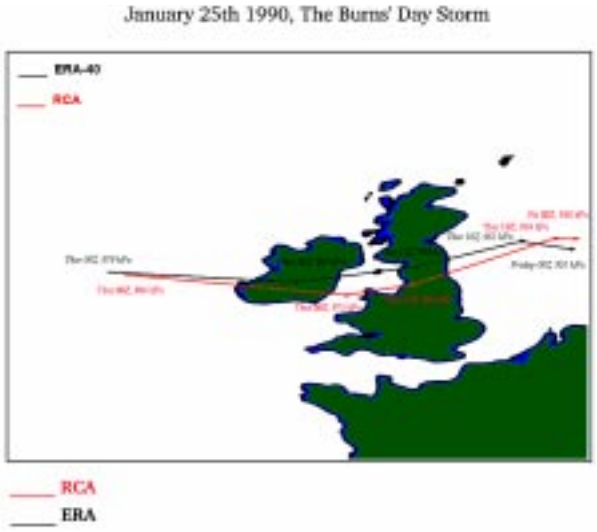

Figure 6.9. Tracks of the Burns' Day storm from ERA-40 (black arrows) and the Regional Climate Model (red arrows) from 00 UTC 25 January 1990 to 00 UTC 26 January 1990.

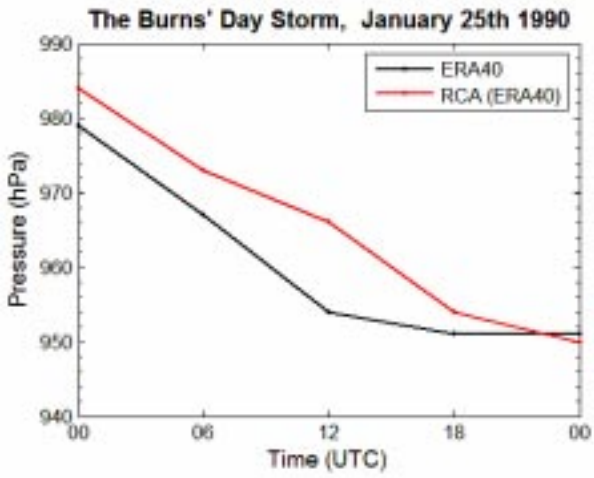

Figure 6.10. Core-pressure values of the Burns' Day storm from ERA-40 and the Regional Climate Model for the period 00 UTC 25 January 1990 to 00 UTC 26 January 1990.

Figure 6.11 shows the frequency of lows as a function of core-pressure value for both sets of data. The differences between the simulations are generally small but for the higher core-pressure values the number of cyclones in the future simulation is slightly less compared with the reference simulation.

Figure 6.12 shows the seasonal and spatial distribution of lows with a core pressure of less than 1000 hPa. Again, the differences between the simulations are small and

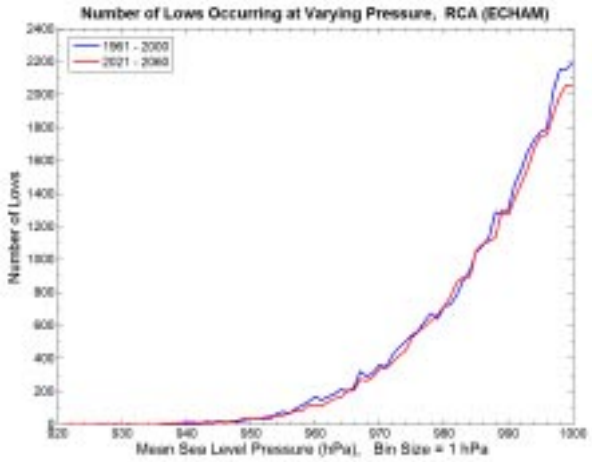

Figure 6.11. Number of lows as a function of core-pressure value for the reference 1961–2000 (blue line) and future 2021–2060 (red line) simulations.

similar results are found when the core-pressure threshold is reduced to 960 hPa.

However, with a core-pressure threshold of 950 hPa a different pattern emerges (Fig. 6.13). Even if there is a substantial decadal variability (Fig. 6.13a), there are at least three peaks in the annual number of lows in the future simulation, which exceed all the peaks in the reference simulation. Furthermore, the intense storms are more frequent in winter and spring (Fig. 6.13b), whereas there is a substantial decrease in autumn. Although the spatial distributions are similar (Fig. 6.13c), the future simulation shows more of these intense cyclones in the south-east quadrant, which is the quadrant with the highest land proportion and therefore more important in terms of impacts. In the future simulation, the storm tracks also extend further south relative to the reference simulation (Fig. 6.14).

6.4 Conclusions

The RCM has been shown to realistically reproduce the frequency and intensity of cyclones in the current climate. The number of intense cyclones with core pressures of less than 950 hPa is very well captured by the model.

Comparison of results for the reference (1961–2000) and future (2021–2060) simulations show that for cyclones with core pressures less than 1000 hPa the total numbers and the seasonal and spatial distributions are similar during both periods. However, the frequency of very intense cyclones with core pressures less than 950 hPa,

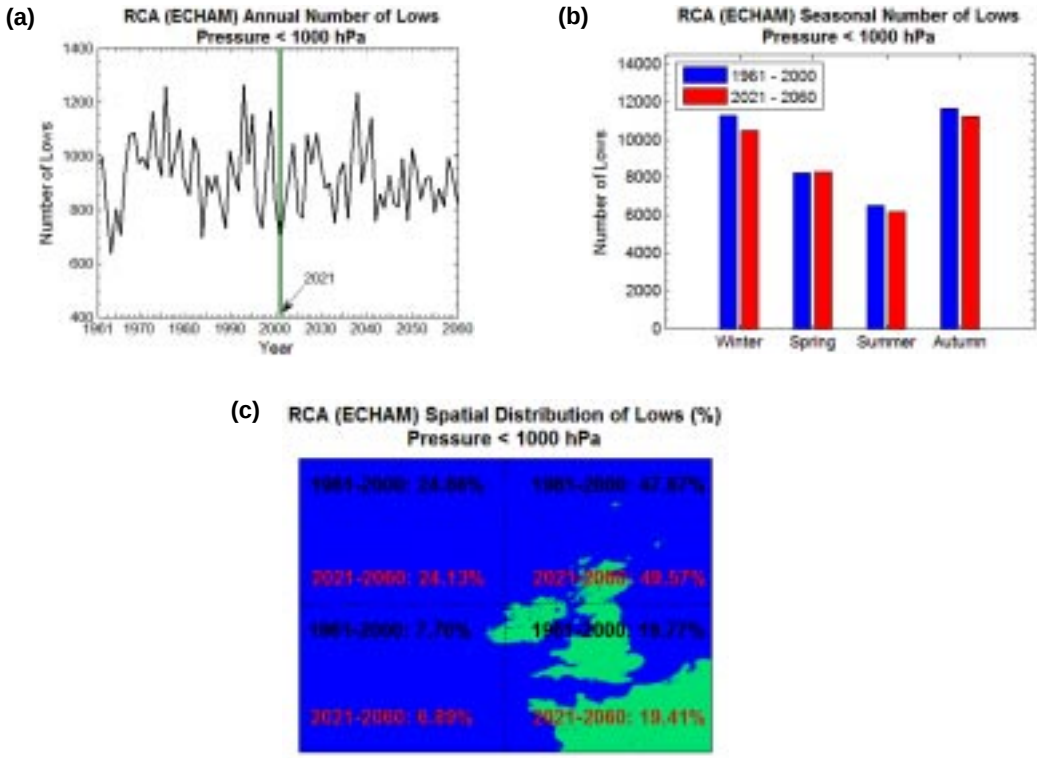

Figure 6.12. (a) Annual, (b) seasonal and (c) spatial distribution of the number of lows with a core pressure of less than 1000 hPa for 1961–2000 and 2021–2060 as simulated by the Regional Climate Model driven by ECHAM4 data.

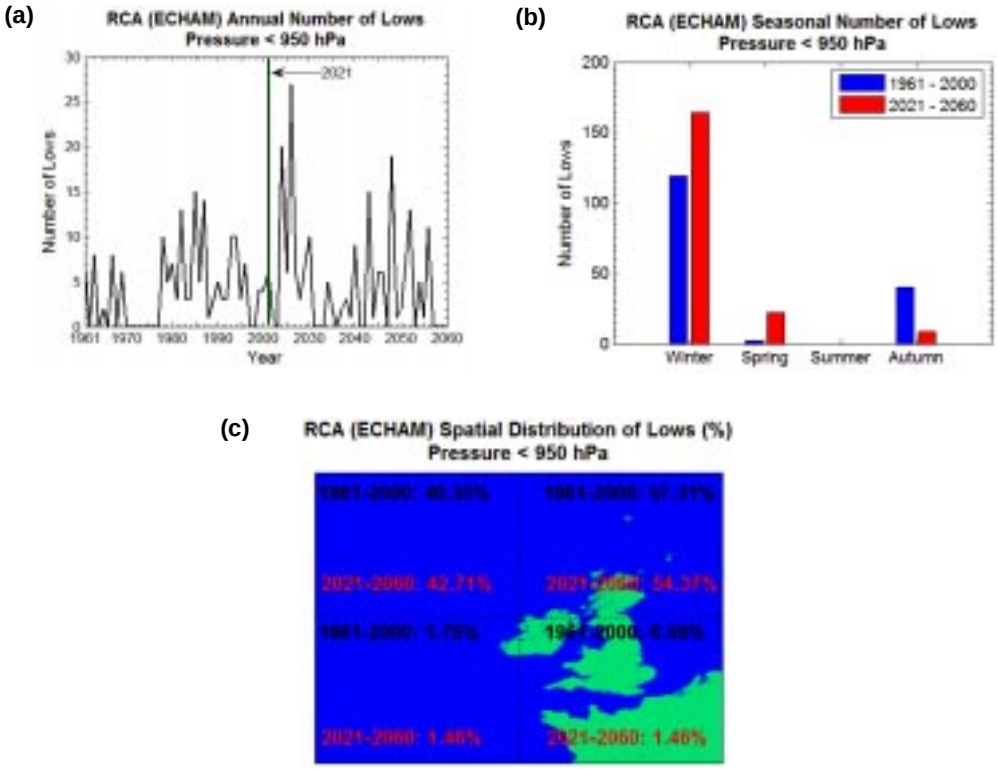

Figure 6.13. (a) Annual, (b) seasonal and (c) spatial distribution of the number of lows with a core pressure of less than 950 hPa for 1961–2000 and 2021–2060 as simulated by the Regional Climate Model driven by ECHAM4 data.

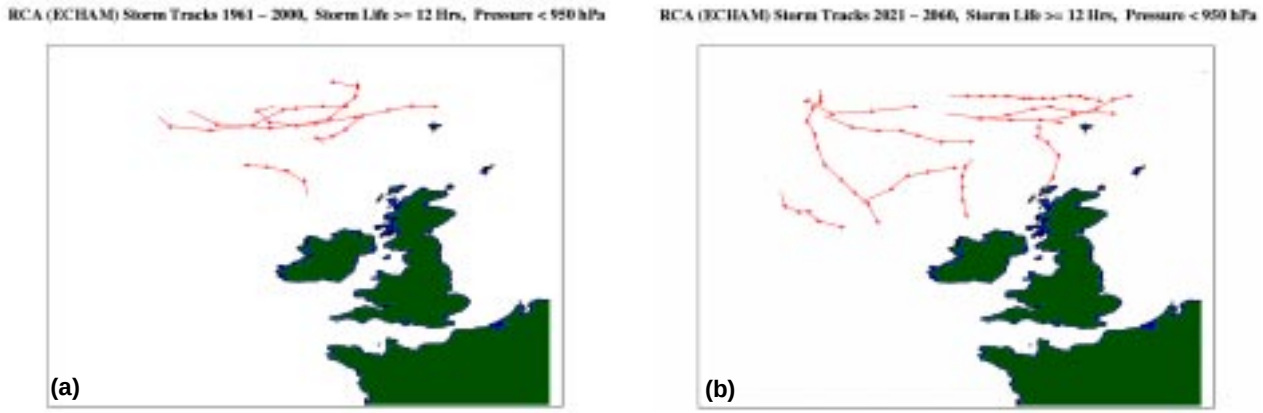

Figure 6.14. Tracks of storms with a core pressure of less than 950 hPa and with a lifetime of at least 12 h from the Regional Climate Model driven by ECHAM4 data for (a) the period 1961–2000 and (b) the period 2021–2060. Arrows show the direction of movement of individual storms.

shows substantial changes: a 15% increase in the future simulation with even stronger increases in winter and spring. Only the autumn numbers show a decrease. Previous studies on cyclone activity in the North Atlantic region show different results for the total number of lows: Zhang and Wang (1997) and Lambert (1995) found a decrease; König *et al.* (1993) found no significant changes; Hall *et al.* (1994) and Sinclair and Watterson (1999) found an increase. However, the increased intensity of cyclones in the future climate of the North Atlantic area close to Ireland and the UK during the winter months is a common feature in these studies (e.g. Lambert, 1995; Geng and Sugi, 2003). In terms of impacts, it is interesting to note that in the future simulation the very intense cyclones (core pressures below 950 hPa) extend further south relative to the reference simulation (Fig. 6.14).

References

ACIA, 2005. *Impacts of a Warming Arctic – Arctic Climate Impact Assessment.* Cambridge University Press, Cambridge, UK, 144 pp.

Arnell, N.W., 2003. Relative effects of multi-decadal climatic variability and changes in the mean and variability of climate due to global warming: future streamflow in Britain. *Journal of Hydrology* **270:** 195–213.

Bergstrom, S., 1995. The HBV model. *In: Computer Models of Watershed Hydrology*, Chapter 13. Water Resources Publications. pp. 443–476.

Bergstrom, S., Carlsson, B., Gardelin, M., Lindstrom, G., Pettersson, A. and Rummukainen, M., 2001. Climate change impacts on the runoff in Sweden – assessments by global climate models, dynamical downscaling and hydrological modelling. *Climate Research* **16:** 101–112.

Chen, G.T.J., Jiang, Z.H. and Wu, M.C., 2003. Spring heavy rain events in Taiwan during warm episodes and the associated large-scale conditions. *Monthly Weather Review* **131:** 1173–1188.

Davies, J.R., Kelly, M.P. and Osborn, T., 1997. Explaining the climate of British Isles. *In:* Hulme, M. and Barrow, E. (eds) *Climates of British Isles: Present, Past and Future.* Springer, Berlin. pp. 386–406.

Geng, Q. and Sugi, M., 2003. Possible change of extratropical cyclone activity due to enhanced greenhouse gases and sulfate aerosols – study with a high-resolution AGCM. *Journal of Climate* **16:** 2262–2274.

Hall, N.M.J., Hoskins, B.J., Valdes, P.J. and Senior, C.A., 1994. Storm tracks in a high-resolution GCM with doubled carbon dioxide. *Quarterly Journal of the Royal Meteorological Society* **120:** 1209–1230.

Horel, J.D., 1981. A rotated principal component analysis of the interannual variability of the Northern Hemisphere 500-mb height field. *Monthly Weather Review* **109:** 2080–2092.

Hurrell, J.W., 1995. Decadal trends in the North Atlantic Oscillation: Regional temperature and precipitation. *Science* **269:** 676–679.

IPCC, 2001. *Climate Change 2001: The Scientific Basis. Contributions of Working Group I to the Third Assessment Report of the Intergovernmental Panel on Climate Change.* Houghton, J.T., Ding, Y., Griggs, D.J., Noguer, M., van der Linden, P.J., Dai, X., Maskell, K. and Johnson, C.A. (eds). Cambridge University Press, Cambridge, UK, 881 pp.

IPCC, 2000. *Special Report on Emission Scenarios. A Special Report of Working Group III of the Intergovernmental Panel on Climate Change.* Nakicenovic, N. and Swart, S. (eds). Cambridge University Press, Cambridge, UK, 599 pp.

Jolliffe, I.T., 1987. Rotation of principal component: some comments. *Journal of Climatology* **7:** 507–510.

Kawamura, R., 1994. A rotated EOF analysis of global sear surface temperature variability with interannual and interdecadal scales. *Journal of Physical Oceanography* **24:** 707–715.

Keane, T. and Collins, J.F., 2004. *Climate, Weather and Irish Agriculture.* pp. 27–62.

Kiely, G., 1999. Climate change in Ireland from precipitation and streamflow observation. *Advances in Water Resources* **23:** 141–151.

Kiely, G., Albertson, J.D. and Parlange, M.B., 1998. Recent trends in diurnal variation of precipitation at Valentia on the west coast of Ireland. *Journal of Hydrology* **207:** 270–279.

König, W., Sausen, R. and Sielmann, F., 1993. Objective identification of cyclones in GCM simulations. *Journal of Climate* **6:** 2217–2231.

Lambert, S.J., 1995. The effect of enhanced greenhouse warming on winter cyclone frequencies and strengths. *Journal of Climate* **8:** 1447–1452.

Lindstrom, G., Johansson, B., Persson, M., Gardelin, M. and Bergstrom, S., 1997. Development and test of the distributed HBV-96 model. *Journal of Hydrology* **201:** 272–288.

Logue, J.J., 1984. Regional variation in the annual cycle of rainfall in Ireland as revealed by principal component analysis. *Journal of Climatology* **4:** 597–607.

McElwain, L. and Sweeney, J., 2003. Climate change in Ireland – recent trends in temperature and precipitation. *Irish Geography* **36:** 97–111.

McKay, M.D., Conover, W.J. and Beckman, R.J., 1979. A comparison of three methods for selection values of input variables in the analysis of output from a computer code. *Technometrics* **2:** 239–245.

Moses, T., Kiladis, G.N., Diaz, H.F. and Barry, R.G., 1987. Characteristics and frequency of reversals in mean sea level pressure in the North Atlantic sector and their relationship to long-term temperature trends. *Journal of Climatology* **7:** 13–30.

Namias, J., 1964. Seasonal persistence and recurrence of European blocking during 1958–1960. *Tellus* **16:** 394–407.

Pilling, C.G. and Jones, J.A.A., 2002. The impact of future climate change on seasonal discharge, hydrological processes and extreme flows in the Upper Wye experimental catchment, mid-Wales. *Hydrological Processes* **16:** 1201–1213.

Rex, D.F., 1951. The effect of Atlantic blocking action upon European climate. *Tellus* **3:** 100–112.

Richman, M.B., 1986. Rotation of principal component. *Journal of Climatology* **6:** 293–335.

Richman, M.B., 1987. Rotation of principal component: a reply. *Journal of Climatology* **7:** 511–520.

Roeckner, E., Arpe, K., Bengsson, L., Christoph, M., Claussen, M., Duemenil, L., Esch, M., Giorgetta, M., Schlese, U. and Schulzweida, U., 1996. The Atmospheric General Circulation Model ECHAM-4: Model Description and Simulation of Present-Day-Climate. Max Planck Institute for Meteorology, Report No. 218, Hamburg, Germany, 90 pp.

Rogers, J.C., 1985. Atmospheric circulation changes associated with the warming over the northern North Atlantic in the 1920s. *Journal of Climate and Applied Meteorology* **24:** 1303–1310.

Rummukainen, M., Raisanen, J., Bringfelt, B., Ullerstig, A., Omstedt, A., Willen, U., Hansson, U. and Jones, C., 2001. A regional climate model for Northern Europe: Model description and results from the downscaling of two GCM control simulations. *Climate Dynamics* **17:** 339–359. DOI: 10.1007/s003820000109.

Schulz, J., Meywerk, J., Ewald, S. and Schluessel, P., 1997. Evaluation of satellite-derived latent heat fluxes. *Journal of Climate* **10:** 2782–2795.

Sinclair, M.R. and Watterson, I.G., 1999. Objective assessment of extratropical weather systems in simulated climates. *Journal of Climate* **12:** 3467–3485.

Stanhill, G., 1998. Long-term trends in, and spatial variation of, solar irradiances in Ireland. *International Journal of Climatology* **18:** 1015–1030.

Sweeney, J., Donnelly, A., McElwain, L. and Jones, M., 2002. *Climate Change Indicators for Ireland.* ERTDI Report Series No. 2. EPA, Wexford.

Sweeney, J., Brereton, T., Byrne, C., Charlton, R., Emblow, C., Fealy, R., Holden, N., Jones, M., Donnelly, A., Moore, S., Purser, P., Byrne, K., Farrell, E., Mayes, E., Minchin, D., Wilson, J. and Wilson, J., 2003. *Climate Change Scenarios and Impacts for Ireland.* ERTDI Report Series No. 15. EPA, Wexford.

Torrence, C. and Compo, G.P., 1998. A practical guide to wavelet analysis. *Bulletin of the American Meteorological Society* **79(1):** 61–78.

Uppala, S.M., Kållberg, P.W., Simmons, A.J., Andrae, U., da Costa Bechtold, V., Fiorino, M., Gibson, J.K., Haseler, J., Hernandez, A., Kelly, G.A., Li, X., Onogi, K., Saarinen, S., Sokka, N., Allan, R.P., Andersson, E., Arpe, K., Balmaseda, M.A., Beljaars, A.C.M., van de Berg, L., Bidlot, J., Bormann, N., Caires, S., Dethof, A., Dragosavac, M., Fisher, M., Fuentes, M., Hagemann, S., Hólm, E., Hoskins, B.J., Isaksen, L., Janssen, P.A.E.M., McNally, A.P., Mahfouf, J.-F., Jenne, R., Morcrette, J.-J., Rayner, N.A., Saunders, R.W., Simon, P., Sterl, A., Trenberth, K.E., Untch, A., Vasiljevic, D., Viterbo, P. and Woollen, J., 2005. The ERA-40 reanalysis. *Quarterly Journal of the Royal Meteorological Society* Submitted.

Wilby, R.C., O'Hare, G. and Barnsley, N., 1997. The North Atlantic Oscillation and British Isles climate variability, 1865–1996. *Weather* **52:** 266–27.

Yu, P.S., Yang, T.Ch. and Chen, S.J., 2001. Comparison of uncertainty analysis methods for a distributed rainfall runoff model. *Journal of Hydrology* **244:** 43–59.

Zhang, Y. and Wang, W.-C., 1997. Model-Simulated Northern Winter Cyclone and Anticyclone Activity under a Greenhouse Warming Scenario. *Journal of Climate* **10:** 1616–1634.

Glossary of Terms

CosmoGrid Network of distributed computing resources in Ireland (see www.CosmoGrid.ie)

ECHAM4 European Centre Hamburg Model Version 4. Global climate model developed at the Max Planck Institute for Meteorology in Hamburg, Germany

ECMWF European Centre for Medium-Range Weather Forecasting

ERA-40 Re-analysis project of the European Centre for Medium-Range Weather Forecasting; archive of re-analysis data

GCM Global Climate Model (also General Circulation Model)

HBV Hydrological discharge model

HOAPS Hamburg Ocean Atmosphere Parameters and Fluxes from Satellite Data. A satellite-derived global climatology of freshwater flux (see www.hoaps.zmaw.de), produced by the Meteorological Institute of the University of Hamburg and the Max Planck Institute for Meteorology in Hamburg

IPCC Intergovernmental Panel on Climate Change

RCM Regional Climate Model

SMHI Swedish Meteorological and Hydrological Institute

SRES Special Report on Emissions Scenarios. The ECHAM4/OPYC3 simulation uses the SRES-B2 scenario, a scenario of moderately increasing greenhouse gas concentrations, for the period 1990–2100. For further details, see www.grida.no/climate/ipcc/emission/095.htm

SST Sea Surface Temperature

T159 Refers to the resolution of the global ERA-40 data in spherical harmonic format. Triangular truncation at wave number 159 corresponds to grid point resolutions of approximately 1.125 degrees. ECHAM4 data have a native horizontal resolution of approximately 2.8 degrees (T42)

UKCIP UK Climate Impacts Programme. Resource provides gridded observation data for elements such as temperature and precipitation

UNFCCC United Nations Framework Convention on Climate Change

Appendix I: Climate Modelling – Background

A1.1 Regional Climate Modelling – Why We Need It

Climate is how weather acts over many years. It includes all the features that we associate with the weather ,such as temperature, wind patterns and precipitation. We can measure our climate by observing and recording the essential details of the environment but to understand the forces that shape the climate system, and to enable us to predict future change, we need a climate model. The model is a numerical description of the processes that influence the climate. As the atmosphere and oceans are the main driving forces for climate, the model needs to have a global perspective if it is to be realistic. Translated into a complex suite of software, the model is run on a computer to simulate the real climate.

Unfortunately, even with today's enormously powerful computer systems, it is a challenging task to develop and run models that track the myriad processes in the atmosphere, ocean- and terrestrial-based ecosystems, that make up the climate. The numerical models process information on a three-dimensional grid but both the time taken to run the model and the memory resources it requires grow rapidly with the number of grid points. A fine grid will provide more detail than a coarser grid but the computational cost may be prohibitive. Currently, the general circulation models (GCMs) describing the atmosphere, coupled with an oceanic counterpart, provide information on grids with a horizontal spacing of typically 100–300 km.

The GCM projections are obviously of interest to planners and developers but ,for many applications, the information does not have sufficient detail. If you are planning a low-lying housing development in a river catchment area, for example, the issue of local flooding is highly pertinent but if the nearest grid point of the GCM is located 100 km away the information it supplies may not be particularly useful. One way to fill the gap is to use a regional climate model (RCM). In a sense, the regional model acts like a magnifying glass to coax extra detail out of the GCM. With the attention on a localised area, marked out with a much

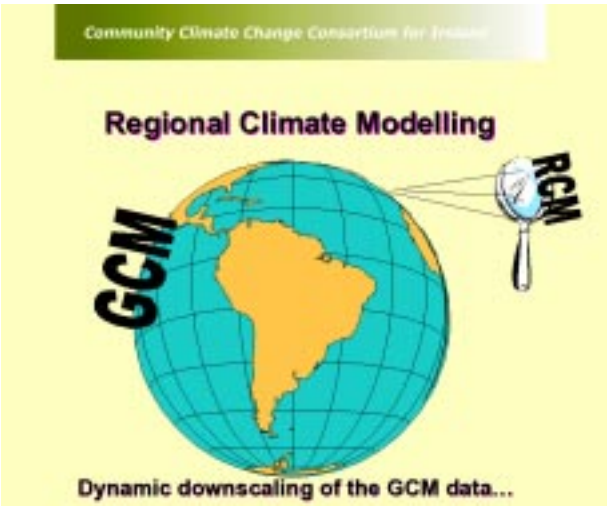

finer grid than the global model, the GCM data are streamed through the area boundaries and in the process they adjust (dynamically downscale) to the finer grid and finer surface details. Because the regional model does not have the entire globe to handle, the computational burden is greatly reduced and horizontal resolutions of 10–15 km can be employed.

Ideally, the flow of information through the lateral boundaries of the Regional Climate Model should be unhindered ('transparent' boundaries) but this is difficult to achieve; the boundaries are a source of noise that must be controlled by the model. Normal practice is to ensure that the area used by the regional model is sufficiently large so that the boundaries are well away from the area of interest (Ireland). The large-scale features of the GCM data should not be altered by the regional model; its purpose is to extract the smaller-scale details. However, this capability may be compromised if the regional area is too large. The choice of a suitable area is based on subjective assessment and judicious experimentation. For computational economy, it is also desirable to have the area as small as possible.

The RCM used by C4I was largely developed under the HIRLAM project, with Met Éireann as a partner, and was further developed for climate work by the Rossby Centre in Sweden, with contributions from C4I.

A1.2 RCM – Vertical Levels

The C4I Regional Climate Model has 40 vertical levels that hug the surface in the lower atmosphere but that flatten out higher up. The two lowest levels are at 35 m and 112 m above the surface, respectively; the top level is at 10 hPa (around 31 km). The plot below shows the approximate heights (in kilometres) and the layout of the model levels in the vicinity of a typical mountain.

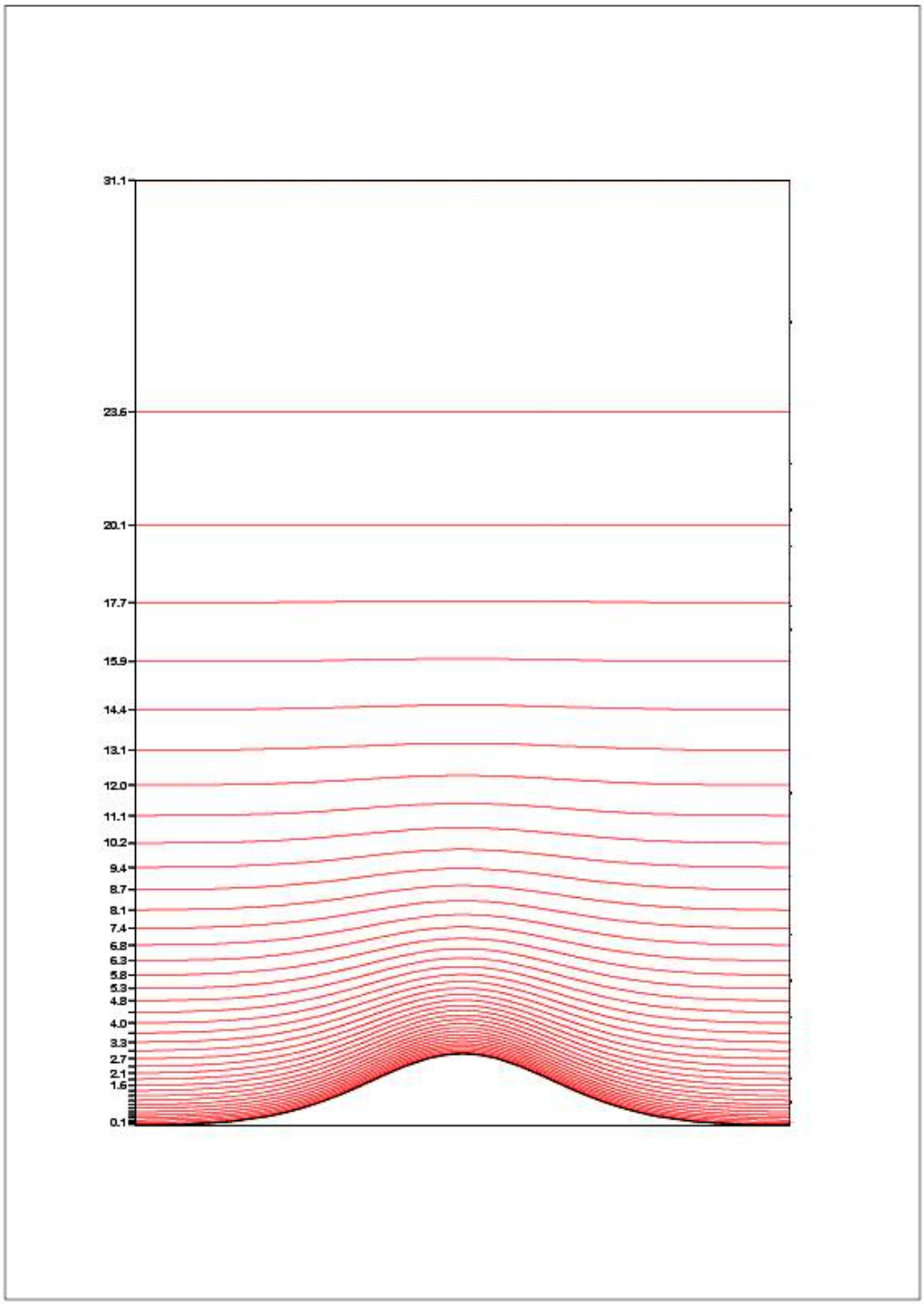

Appendix II: Data Sets in Regional Climate Modelling

A2.1 Local Observations

An extensive set of meteorological observations are available from Met Éireann. Most of the data are surface based but upper-air sounding data for Valentia Observatory are also available; additional data for Northern Ireland are available from the ECMWF observation archive. The UKCIP data sets represent interpolated surface observation data on a 5-km grid covering the land area; they are particularly useful for validating the output data from the Regional Climate Model (also on a grid).

A2.2 Re-analysis Data (ERA-40)

The quality and density of meteorological observations are important issues in the detection of climate change; a lack of observations will make it difficult to derive the average weather in a region while the information will be flawed if the quality of the data is poor. The ERA-40 project was set up to provide the most accurate three-dimensional descriptions of the atmosphere based on available observations. The impact of inhomogeneities in observation coverage and observation quality are reduced by using state-of-the-art atmospheric models. Model output consists of numerous weather parameters on a three-dimensional global grid at 6-h frequency covering the period from September 1957 to August 2002. The data, regarded as providing an accurate measure of the true state of the atmosphere, are ideal for validating regional climate models.

A2.3 Satellite Data: HOAPS

Remote sensing is the technology of observing the Earth from space. The microwave radiation radiated naturally from the Earth's surface and atmosphere is rich with information about the atmosphere (temperature, humidity, clouds, and rain) and the surface (temperature, vegetation, roughness, and moisture). Since microwaves can penetrate clouds, surface characteristics can be measured from space even when clouds are present. The Special Sensor Microwave Imager (SSM/I) is a passive microwave radiometer flown aboard the American polar orbiting DMSP satellites for retrieving this information.

HOAPS (Hamburg Ocean Atmosphere Parameters and Fluxes from Satellite Data) is a global climatology of sea surface parameters, surface energy and freshwater fluxes, derived from satellite radiances for the time period July 1987 to December 1998. It was produced by the Meteorological Institute of the University of Hamburg and the Max Planck Institute for Meteorology in Hamburg. The SSM/I and the Advanced Very High Resolution Radiometer (AVHRR) data from the satellites were used to derive global fields of surface meteorological and oceanographic parameters. The archive contains information on latent heat flux, evaporation, precipitation and net freshwater flux over ice-free ocean areas for various averaging periods and grid sizes.

Appendix III List of Meteorological Products Generated by the Regional Climate Model

Output products available from the RCM simulations are listed below:

- Geopotential at surface, 150, 500, 850, 925 and 1000 hPa
- Temperature at surface and 2 m, and at 150, 500, 850, 925 and 1000 hPa
- 3-h maximum and minimum surface and 2-m temperature
- 2-m dew-point temperature
- Temperature at three depths
- Wind at 10 m, 60 m, and at 150, 500, 850, 925 and 1000 hPa
- Maximum (3-h) 10-m wind
- Surface friction velocity
- Relative humidity at 2 m, and at 150, 500, 850, 925 and 1000 hPa
- 2-m specific humidity
- Mean sea level pressure
- Total, large-scale and convective precipitation
- Soil moisture at three depths
- Water run-off at two depths
- Total cloud cover
- Vertically integrated cloud liquid water and water vapour
- Cloud top temperature (infrared)
- Cloud water reflectivity (visible)
- Water vapour brightness temperature and correction for clouds
- Freezing height
- Planetary boundary layer height
- Averaged surface sensible, latent and momentum heat flux
- Averaged surface short-wave and long-wave radiation
- Averaged upward and downward short-wave and long-wave radiation at surface and top of the atmosphere.

Appendix IV: Greenhouse Gas Emission Scenarios

Future levels of greenhouse gases are based on plausible 'storylines' of future development. Each storyline is associated with a projected emission pattern that can be used in climate model simulations. The main storylines, documented in the IPCC Special Report on Emission Scenarios (SRES) (IPCC, 2000), are listed below.

A1. The A1 storyline and scenario family describes a future world of very rapid economic growth, global population that peaks in mid-century and declines thereafter, and the rapid introduction of new and more efficient technologies. Major underlying themes are convergence among regions, capacity building and increased cultural and social interactions, with a substantial reduction in regional differences in *per capita* income. The A1 scenario family develops into three groups that describe alternative directions of technological change in the energy system. The three A1 groups are distinguished by their technological emphasis: fossil intensive (A1FI), non-fossil energy sources (A1T), or a balance across all sources (A1B) (where balanced is defined as not relying too heavily on one particular energy source, on the assumption that similar improvement rates apply to all energy supply and end-use technologies).

A2. The A2 storyline and scenario family describes a very heterogeneous world. The underlying theme is self-reliance and preservation of local identities. Fertility patterns across regions converge very slowly, which results in a continuously increasing population. Economic development is primarily regionally oriented and *per capita* economic growth and technological change more fragmented and slower than other storylines.

B1. The B1 storyline and scenario family describes a convergent world with the same global population, that peaks in mid-century and declines thereafter, as in the A1 storyline, but with rapid change in economic structures toward a service and information economy, with reductions in material intensity and the introduction of clean and resource-efficient technologies. The emphasis is on global solutions to economic, social and environmental sustainability, including improved equity, but without additional climate initiatives.

B2. The B2 storyline and scenario family describes a world in which the emphasis is on local solutions to economic, social and environmental sustainability. It is a world with a continuously increasing global population, at a rate lower than A2, intermediate levels of economic development, and less rapid and more diverse technological change than in the B1 and A1 storylines. While the scenario is also oriented towards environmental protection and social equity, it focuses on local and regional levels.